NASA/CR-2002-211648
ICASE Report No. 2002-13

Analysis of Boundary Conditions for Factorizable Discretizations of the Euler Equations

Boris Diskin
ICASE, Hampton, Virginia

James L. Thomas
NASA Langley Research Center, Hampton, Virginia

May 2002

The NASA STI Program Office . . . in Profile

Since its founding, NASA has been dedicated to the advancement of aeronautics and space science. The NASA Scientific and Technical Information (STI) Program Office plays a key part in helping NASA maintain this important role.

The NASA STI Program Office is operated by Langley Research Center, the lead center for NASA's scientific and technical information. The NASA STI Program Office provides access to the NASA STI Database, the largest collection of aeronautical and space science STI in the world. The Program Office is also NASA's institutional mechanism for disseminating the results of its research and development activities. These results are published by NASA in the NASA STI Report Series, which includes the following report types:

- TECHNICAL PUBLICATION. Reports of completed research or a major significant phase of research that present the results of NASA programs and include extensive data or theoretical analysis. Includes compilations of significant scientific and technical data and information deemed to be of continuing reference value. NASA's counterpart of peer-reviewed formal professional papers, but having less stringent limitations on manuscript length and extent of graphic presentations.

- TECHNICAL MEMORANDUM. Scientific and technical findings that are preliminary or of specialized interest, e.g., quick release reports, working papers, and bibliographies that contain minimal annotation. Does not contain extensive analysis.

- CONTRACTOR REPORT. Scientific and technical findings by NASA-sponsored contractors and grantees.

- CONFERENCE PUBLICATIONS. Collected papers from scientific and technical conferences, symposia, seminars, or other meetings sponsored or cosponsored by NASA.

- SPECIAL PUBLICATION. Scientific, technical, or historical information from NASA programs, projects, and missions, often concerned with subjects having substantial public interest.

- TECHNICAL TRANSLATION. English-language translations of foreign scientific and technical material pertinent to NASA's mission.

Specialized services that complement the STI Program Office's diverse offerings include creating custom thesauri, building customized data bases, organizing and publishing research results . . . even providing videos.

For more information about the NASA STI Program Office, see the following:

- Access the NASA STI Program Home Page at ***http://www.sti.nasa.gov***

- Email your question via the Internet to help@sti.nasa.gov

- Fax your question to the NASA STI Help Desk at (301) 621-0134

- Telephone the NASA STI Help Desk at (301) 621-0390

- Write to:
  NASA STI Help Desk
  NASA Center for AeroSpace Information
  7121 Standard Drive
  Hanover, MD 21076-1320

NASA/CR-2002-211648
ICASE Report No. 2002-13

Analysis of Boundary Conditions for Factorizable Discretizations of the Euler Equations

Boris Diskin
ICASE, Hampton, Virginia

James L. Thomas
NASA Langley Research Center, Hampton, Virginia

ICASE
NASA Langley Research Center
Hampton, Virginia

Operated by Universities Space Research Association

Prepared for Langley Research Center
under Contract NAS1-97046

May 2002

Available from the following:

NASA Center for AeroSpace Information (CASI)
7121 Standard Drive
Hanover, MD 21076-1320
(301) 621-0390

National Technical Information Service (NTIS)
5285 Port Royal Road
Springfield, VA 22161-2171
(703) 487-4650

ANALYSIS OF BOUNDARY CONDITIONS FOR FACTORIZABLE DISCRETIZATIONS OF THE EULER EQUATIONS

BORIS DISKIN* AND JAMES L. THOMAS†

Abstract. In this article, several sets of boundary conditions for factorizable schemes corresponding to the steady-state compressible Euler equations are evaluated. The analyzed model is a one-dimensional constant-coefficient problem. Numerical tests have been performed for a fully subsonic quasi-one-dimensional flow in a convergent/divergent channel.

This paper focuses on the effect of boundary-condition equations on stability and accuracy of the discrete solutions. Explicit correspondence between solutions and boundary conditions is established through a boundary-condition-sensitivity (**BCS**) matrix. The following new findings are reported:

(1) Examples of stable discrete problems contradicting a wide-spread belief that employment of a one-order-lower approximation schemes in an $O(h)$-small region does not affect the overall accuracy order of the solution have been found and explained. Such counterexamples can only be constructed for *systems* of differential equations. For scalar equations, the conventional wisdom is correct.

(2) A negative effect of overspecified (although, exact) boundary conditions on accuracy and stability of the solution has been observed and explained.

(3) Sets of practical boundary conditions for factorizable schemes providing stable second-order accurate solutions have been formulated. These schemes belong to a family of second-order schemes requiring second-order accuracy for some numerical-closure boundary conditions.

Key words. compressible Euler equations, factorizable discretization scheme, practical boundary conditions, I-stability, B-stability

Subject classification. Applied and Numerical Mathematics

1. Introduction. An efficiency goal for the new generation of multigrid flow solvers is to arrive at solutions of the governing system of equations in a total computational work that is a small (less than 10) multiple of the operation count in one target-grid residual evaluation. Such efficiency is defined as textbook multigrid efficiency (TME) [4, 5]. TME has been achieved for elliptic problems long ago [1, 2, 3, 6]. The difficulties associated with extending TME for solution of the Navier-Stokes equations relate to the fact that the Navier-Stokes equations are a system of coupled nonlinear equations that is not fully elliptic, even for subsonic Mach numbers, but contains hyperbolic partitions. TME for the Navier-Stokes simulations can be achieved if different factors contributing to the system could be separated and treated optimally, e.g., by multigrid for elliptic factors and by downstream marching for hyperbolic factors. An efficient way to separate the factors is the *distributed relaxation* approach proposed in [2, 3]. The general framework for achieving TME in large-scale computational fluid dynamics (CFD) applications has been discussed in [8, 20].

Design of a distributed relaxation scheme for Navier-Stokes systems can be significantly simplified if the target discretization possesses two properties:

*ICASE, Mail Stop 132C, NASA Langley Research Center, Hampton, Virginia 23681 (email: bdiskin@icase.edu). This research was supported by the National Aeronautics and Space Administration under NASA Contract No. NAS1-97046 while the author was in residence at ICASE, NASA Langley Research Center, Hampton, Virginia 23681.

†Computational Modeling and Simulation Branch, Mail Stop 128, NASA Langley Research Center, Hampton, VA 23681 (email: j.l.thomas@larc.nasa.gov).

(1) The discretization of the corresponding principally linearized system $\mathbf{L}$ is *factorizable* [3, 4, 12, 16, 17], i.e., the discrete system determinant can be represented as a product of discrete scalar factors, each of them approximating a corresponding factor of the determinant of the *differential* Navier-Stokes equations.

(2) The obtained scalar factor discretizations are stable, easily solvable, and reflect the physical anisotropies.

Some well-known discrete schemes are naturally factorizable, e.g., the staggered-grid discretization scheme for incompressible flow dating back to the mid 60's [13, 14, 15]. However, the majority of discrete schemes in current use are not factorizable. Even for factorizable schemes, the discretizations obtained for scalar factors of the determinant are not often stable or/and have wrong strong-anisotropy directions. The search for new factorizable discretization schemes is chiefly motivated by the need to derive discrete schemes with the resulting discretizations of scalar factors satisfying some desired properties (e.g., stability, correct alignment with the physical anisotropies, compactness, availability of an efficient relaxation scheme, etc.) Recently, two families of factorizable discretization schemes for the compressible Euler equations have emerged [12, 16].

The original paper [12] has demonstrated TME in solving factorizable discretizations of the compressible Euler equations with solution values at the boundary and, wherever necessary, outside of the target computational domain overspecified from the known exact solution of the differential problem. This formulation is very attractive because it bypasses difficulties associated with boundary conditions and facilitates TME demonstration. However, overspecified boundary conditions are impractical; usually, the boundary data are not available outside of the computational domain and even at the boundaries the data are incomplete and/or accurate only to some finite precision that might depend on the mesh. Multigrid considerations make the overspecified boundary conditions even less viable: on coarse grids, specification of data located far beyond the target computational domain is required. This paper studies more practical boundary conditions for the factorizable discretization schemes introduced in [12].

In general, boundary conditions for a discrete problem may include two components: the physical boundary conditions and the numerical-closure equations. The former are discrete approximations to the boundary conditions of the target differential problem. The latter are special discrete approximations (different from the interior approximations) to the differential equations usually defined within an $O(h)$-small boundary neighborhood.

This paper focuses on the effect of boundary-condition equations on stability of the discrete solutions. For steady-state discrete problems, there are two relevant types of stability: (A) stability of difference approximations to differential operators and (B) stability of discrete solutions with respect to boundary data. Because the first type of stability describes the properties of the *interior* approximations it is referenced in this paper as I-stability; the second type of stability is referenced as B-stability.

For a discrete operator $\mathbf{L^h}$ approximating the differential constant-coefficient operator $\mathbf{L}$, the property of I-stability can be defined as follows: Let the symbols of the differential operator $\mathbf{L}[u]$ and the discrete operator $\mathbf{L^h}[u]$ be defined as $\mathbf{L}(\bar{\alpha}) = e^{-i(\bar{\alpha}\cdot\mathbf{e})}\mathbf{L}[e^{i(\bar{\alpha}\cdot\mathbf{e})}]$ and $\mathbf{L^h}(\mathbf{w}) = e^{-i(\mathbf{w}\cdot\mathbf{j})}\mathbf{L^h}[e^{i(\mathbf{w}\cdot\mathbf{j})}]$, respectively, where $\mathbf{e} = (x, y, z)$ is a coordinate vector, $\bar{\alpha} = (\alpha_x, \alpha_y, \alpha_z)$ are frequencies of a continuous Fourier component, $\mathbf{j} = (j_x, j_y, j_z)$ are the grid indexes, and $\mathbf{w} = (\omega_x, \omega_y, \omega_z), 0 \le |\omega_x|, |\omega_y|, |\omega_z| \le \pi$ are normalized Fourier frequencies.

Definition of I-stability: The discrete operator $\mathbf{L^h}$ is an I-stable approximation to the differential operator $\mathbf{L}$ if $\mathbf{L^h}(\mathbf{w}) = 0$ implies that $\mathbf{L}(\mathbf{w}/h) = 0$.

This definition of I-stability requires from the discrete operator to have no *global* (Fourier-component)

solutions to the homogeneous discrete equations besides those that are also solutions of the corresponding homogeneous differential equations. Most higher-than-first-order difference approximations admit some spurious solutions that do not approximate the solutions of the differential equations. For I-stable difference approximations, these spurious solutions should be local, i.e., (nearly) vanishing beyond some neighborhood that shrinks to a zero-measure set as the mesh size h tends to zero. In boundary-value problems, the spurious solutions of I-stable difference approximations are usually exponential functions of the grid indexes. These functions represent the discrete boundary layers and fast decrease from the boundary toward the interior. A wide ($2h$) central-differencing approximation to the convection operator ($\bar{a} \cdot \bigtriangledown$), where $\bar{a}$ is a constant vector, represents an I-unstable approximation because the corresponding homogeneous discrete equation admits several solutions: a constant corresponding to a physical constant solution of the differential equation and functions oscillating with the highest normalized frequency π in some (or all) coordinate grid directions. The latter functions represent global spurious discrete solutions with the unit amplitude everywhere in the interior. These discrete solutions do not approximate solutions of the differential equation. Global spurious solutions are not necessarily highly oscillating. Varying the Mach number parameter in the Scheme # 1 from [12], one can easily construct examples of I-unstable approximations with smooth global spurious solutions.

The notion of I-stability is a generalization of the notion of h-ellipticity widely used in multigrid theory. A discrete operator is h-elliptic if the corresponding discrete homogeneous equation does not admit *highly oscillatory* solutions. If the target differential solutions are smooth on a given grid, I-stability implies h-ellipticity.

For constant-coefficient operators, a difference approximation is I-stable if the number of characteristic-polynomial roots with the unit amplitude is equal to the number of linearly independent solutions of the homogeneous differential equation. The number of roots with amplitudes differing from one may be arbitrary. The discrete solutions corresponding to the roots with the unit amplitude are referred as physical solutions. The physical solutions are associated with the physical boundary conditions. The coefficients of the spurious solutions are strongly influenced by the numerical-closure equations. All the difference approximations analyzed in this paper are I-stable.

Let us define the boundary data as known quantities used in formulation boundary conditions, e. g., solution values at the boundary (Dirichlet data), solution derivatives at the boundary (Neumann data), the source functions for the interior equations (numerical-closure data), etc.

Definition of B-stability: A discrete scheme approximating a differential problem is *stable with respect to boundary data* (B-stable) if for any fixed (independent of mesh size h) perturbation of boundary data, the sequence of discrete solutions converges as h tends to zero.

B-stability implies that the discrete scheme remains meaningful even if the boundary data are not precisely specified. Even I-stable difference approximations with physically realistic boundary conditions may become B-unstable. Moreover, B-stability may depend on norms in which solution convergence is considered. Examples of discrete schemes for boundary-value problems that are B-stable in some common integral norms but B-unstable in the L_∞ norm are shown in Section 6.

This paper also represents an attempt to formalize our intuitive understanding of *practical* discrete boundary conditions. Assuming that the target differential problem has a reasonable set of physical boundary conditions and is well posed, the four requirements for practical discrete boundary conditions supplementing an I-stable discrete approximation in the interior are formulated as following:

(1) *Location requirement:* The discretization of physical boundary conditions should be specified at the boundary.

(2) *Well-posedness requirement:* The obtained discrete problem should be well posed, i.e., possess a unique solution (on a given grid) continuously dependent on the problem data.

(3) *B-stability requirement:* The discrete problem should be B-stable.

(4) *Accuracy requirement:* The *accuracy* of the discrete solutions should be determined by the approximation order of the interior discrete equations, i.e., should not deteriorate because of boundary conditions, either the physical or numerical-closure type.

The overspecified boundary conditions, while often leading to well-posed discrete formulations, obviously violate the location requirement (1); what is less obvious, in some cases, they also violate the B-stability (3) and accuracy (4) requirements. Examples are shown in Section 6.

A detailed discrete analysis is employed in this paper to evaluate several sets of boundary conditions. The model is a one-dimensional constant-coefficient problem corresponding to the compressible Euler equations, although the methodology applies to general systems. The interior discretizations are I-stable factorizable schemes derived in [12]. Explicit correspondence between solutions and boundary conditions is established through a boundary-condition-sensitivity (**BCS**) matrix. Analysis of coefficients of the **BCS**matrix provides reliable predictions for B-stability and accuracy of the discrete solutions. The following new findings are reported:

(1) Examples of I-stable discrete problems contradicting a wide-spread belief that employment of a one-order-lower approximation scheme as numerical-closure equations in an $O(h)$-small region does not affect the overall accuracy order of the solution have been found and explained. Such counterexamples can only be constructed for *systems* of differential equations. For scalar equations, the conventional wisdom is correct.

(2) A negative effect of overspecified (although, exact) boundary conditions on accuracy and B-stability of the solution has been observed and explained.

(3) Sets of practical boundary conditions for factorizable schemes of [12] that provide B-stable second-order accurate solutions have been formulated. These schemes belong to a family of second-order schemes requiring second-order accuracy for some numerical-closure boundary conditions.

The material in this paper has been organized in the following order: Section 2 formulates the model differential constant-coefficient problem. A family of factorizable discretizations for the model problem is outlined in Section 3. The discrete solution structure is analyzed in Section 4. Section 5 introduces and illustrates the analysis of discrete boundary conditions. Section 6 defines and analyzes several sets of boundary conditions employed for two factorizable discretizations. The results of numerical tests performed for quasi-one-dimensional compressible subsonic flow in a convergent-divergent channel are reported in Section 7. Section 8 contains concluding remarks as well as directions for future research.

2. Model Problem. The set of the quasi-one-dimensional nonconservative Euler equations is given by

$$\begin{aligned} u\partial_x u + \tfrac{1}{\rho}\partial_x p &= 0, \\ \rho c^2 \partial_x u + u\partial_x p &= -\gamma p u \tfrac{\sigma_x}{\sigma}, \\ (\gamma-1)\epsilon\partial_x u + u\partial_x \epsilon &= -(\gamma-1)\epsilon u \tfrac{\sigma_x}{\sigma}, \end{aligned} \tag{2.1}$$

where $\sigma(x)$ is the area distribution. The pressure p, internal (thermal) energy ϵ, density ρ, and sound speed c are related as

$$p = (\gamma-1)\rho\epsilon, \tag{2.2}$$

$$c^2 = \gamma p/\rho, \tag{2.3}$$

where γ is the ratio of specific heats.

The corresponding model problem

$$\begin{pmatrix} \bar{u}\partial_x & \frac{1}{\rho}\partial_x & 0 \\ \rho c^2 \partial_x & \bar{u}\partial_x & 0 \\ (\gamma-1)\bar{\epsilon}\partial_x & 0 & \bar{u}\partial_x \end{pmatrix} \begin{pmatrix} u \\ p \\ \epsilon \end{pmatrix} = \begin{pmatrix} f_1(x) \\ f_2(x) \\ f_3(x) \end{pmatrix}. \tag{2.4}$$

assumes that the coefficients $\bar{u}, \rho, c$, and $\bar{\epsilon}$ are constants unrelated to the unknown functions (u, p, ϵ). In the subsonic regime, a natural set of boundary conditions is u and ϵ specified at the inflow boundary and p specified at the outflow boundary. With this set of boundary conditions the problem (2.4) is well posed.

The third equation is decoupled from the other equations. Thus, for the purpose of analysis, we can focus on the system of two constant-coefficient equations

$$\mathbf{L}\ \mathbf{q} = \mathbf{f}, \tag{2.5}$$

where

$$\mathbf{L} \equiv \begin{pmatrix} \bar{u}\partial_x & \frac{1}{\rho}\partial_x \\ \rho c^2 \partial_x & \bar{u}\partial_x \end{pmatrix}, \tag{2.6}$$

$\mathbf{q} = (u, p)^T$, and $\mathbf{f} = (f_1, f_2)^T$ The determinant of the matrix operator $\mathbf{L}$ is the full-potential operator

$$\mathcal{F} = \left(\bar{u}^2 - c^2\right) \partial_{xx}. \tag{2.7}$$

3. Factorizable Discretizations. In this section, we briefly consider derivation of factorizable discretizations for the model problem (2.5). Such schemes for the three-dimensional Euler equations have been derived in [12]; generalization to conservative schemes has been discussed in [11].

The starting point is a "basic" collocated-grid discretization, $\mathbf{L^h}_{\text{basic}}$, for the matrix operator $\mathbf{L}$ of (2.6) defined as

$$\mathbf{L^h}_{\text{basic}} = \begin{bmatrix} \bar{u}\partial^u & \frac{1}{\rho}\partial^c \\ \rho c^2 \partial^c & \bar{u}\partial^d \end{bmatrix}, \tag{3.1}$$

where the discrete derivatives, ∂^u, ∂^c, and ∂^d are second-order accurate upwind (upwind-biased), central, and downwind (downwind-biased) difference approximations, respectively. The determinant of $\mathbf{L^h}_{\text{basic}}$ is a discrete approximation to the full-potential operator given by

$$\bar{u}^2 \partial^u \partial^d - c^2 \left(\partial^c\right)^2. \tag{3.2}$$

This discrete approximation is not I-stable for subsonic Much numbers ($M = \bar{u}/c < 1$) and has an incorrect (streamwise) direction of strong coupling for near-sonic Much numbers ($M \approx 1$). An I-stable discrete approximation for the full-potential operator (2.7) would be

$$\mathcal{F}^h = \left(\bar{u}^2 - c^2\right) \partial^h_{xx}, \tag{3.3}$$

where ∂^h_{xx} is an I-stable approximation to the second derivative. A way to achieve I-stability for the discrete full-potential factor is to replace the discretization $\bar{u}\partial^d$ with $\bar{u}\partial^d + \mathcal{A}^h$, so that the discrete full-potential operator is transformed to a desired (I-stable) one. This transformation implies that

$$\mathcal{A}^h = \left(\bar{u}\partial^u\right)^{-1} \mathcal{D}^h, \tag{3.4}$$

$$\mathcal{D}^h = \mathcal{F}^h - \left(\bar{u}^2 \partial^u \partial^d - c^2 \left(\partial^c\right)^2\right), \tag{3.5}$$

where $\mathcal{F}^h$ is a desired discretization of the full-potential operator. Assuming that $\mathcal{F}^h$ is second-order accurate, $\mathcal{A}^h$ is $O(h^2)$-small, and the overall second-order discretization accuracy is not compromised. The operator $\left(\bar{u}\partial^u\right)^{-1}$ is a nonlocal operator and its introduction can be effected through a new auxiliary variable ψ^h and a new discrete equation $\bar{u}\partial^u\psi^h = \mathcal{D}^h p^h$. Finally, a family of factorizable I-stable discretizations for (2.6) is formulated as

$$
\begin{aligned}
r_1(\mathbf{q^h})_j &:= \quad \bar{u}\partial^u u_j^h + \tfrac{1}{\rho}\partial^c p_j^h = f_j^1, \\
r_2(\mathbf{q^h})_j &:= \quad \bar{u}\partial^u \psi_j^h - \mathcal{D}^h p_j^h = 0, \\
r_3(\mathbf{q^h})_j &:= \quad \rho c^2 \partial^c u_j^h + \psi_j^h + \bar{u}\partial^d p_j^h = f_j^2,
\end{aligned}
\tag{3.6}
$$

where $\mathbf{q^h}_j = (u_j^h, \psi_j^h, p_j^h)^T$, $f_j^1 = f_1(jh)$, and $f_j^2 = f_2(jh)$

4. Solutions. Let the exact solution of the differential problem (2.5) defined on the interval $x \in [0,1]$ be

$$
\mathbf{q}_{\text{exact}} = \begin{pmatrix} u_{\text{exact}} \\ p_{\text{exact}} \end{pmatrix} = \begin{pmatrix} C_u \\ C_p \end{pmatrix} e^{i\alpha x}, \tag{4.1}
$$

where α is an arbitrary frequency. Then

$$
\begin{pmatrix} f_1(x) \\ f_2(x) \end{pmatrix} = \begin{pmatrix} \bar{f}_1 \\ \bar{f}_2 \end{pmatrix} e^{i\alpha x}, \qquad \begin{pmatrix} \bar{f}_1 \\ \bar{f}_2 \end{pmatrix} = \begin{pmatrix} \bar{u}C_u + \frac{1}{\rho}C_p \\ \rho c^2 C_u + \bar{u}C_p \end{pmatrix} i\alpha. \tag{4.2}
$$

The corresponding system of discrete equations is

$$
\mathbf{L^h q}^h \equiv \begin{pmatrix} \bar{u}\partial^u & 0 & \frac{1}{\rho}\partial^c \\ 0 & \bar{u}\partial^u & -\mathcal{D}^h \\ \rho c^2 \partial^c & 1 & \bar{u}\partial^d \end{pmatrix} \begin{pmatrix} u^h \\ \psi^h \\ p^h \end{pmatrix} = \begin{pmatrix} f_j^1 \\ 0 \\ f_j^2 \end{pmatrix}, \tag{4.3}
$$

where $j = 1, 2, \ldots, N-1$, $N = 1/h$, $f_j^1 = f_1(jh)$, and $f_j^2 = f_2(jh)$. A discrete representation of the exact solution (4.1) on a grid with mesh size h is given by

$$
\mathbf{q}^h_{\text{exact}} \equiv \begin{pmatrix} u^h_{\text{exact}} \\ \psi^h_{\text{exact}} \\ p^h_{\text{exact}} \end{pmatrix} = \begin{pmatrix} C_u \\ 0 \\ C_p \end{pmatrix} e^{i\omega j}, \tag{4.4}
$$

where $\omega = \alpha h$ is a normalized frequency. The system (4.3) is subject to physical boundary conditions

$$
u_0 = C_u, \qquad \psi_0 = 0, \qquad p_N = C_p e^{i\alpha}. \tag{4.5}
$$

Depending on the choice of difference operators, some numerical-closure equations may be required to complete the discrete formulation. The solution to the problem (4.3), (4.5) can be sought as a combination of a particular solution to the nonhomogeneous system of equations (4.3) and the general solution to the corresponding homogeneous problem (3.6).

A particular solution to (4.3) can be found in the form

$$
\mathbf{q}^h_{\text{par}} \equiv \begin{pmatrix} u^h_{\text{par}} \\ \psi^h_{\text{par}} \\ p^h_{\text{par}} \end{pmatrix} = \begin{pmatrix} \hat{u} \\ \hat{\psi} \\ \hat{p} \end{pmatrix} e^{i\omega j}. \tag{4.6}
$$

$$\begin{pmatrix} \hat{u} \\ \hat{\psi} \\ \hat{p} \end{pmatrix} = \left(\mathbf{L^h}(e^{i\omega})\right)^{-1} \begin{pmatrix} \bar{f}_1 \\ 0 \\ \bar{f}_2 \end{pmatrix}, \tag{4.7}$$

where

$$\mathbf{L^h}(\lambda) = \begin{pmatrix} \bar{u}\partial^u(\lambda) & 0 & \frac{1}{\rho}\partial^c(\lambda) \\ 0 & \bar{u}\partial^u(\lambda) & -\mathcal{D}^h(\lambda) \\ \rho c^2 \partial^c(\lambda) & 1 & \bar{u}\partial^d(\lambda) \end{pmatrix} \tag{4.8}$$

is a generalized symbol of the discrete operator $\mathbf{L^h}$ (4.3). The entries of $\mathbf{L^h}(\lambda)$ are generalized symbols of discrete scalar operators defined as responses of these operators on the exponent function λ^j. For example, the generalized symbol of the central second-order difference approximation to the first derivative is $\partial^c \lambda^j = \partial^c(\lambda)\lambda^j$, $\partial^c(\lambda) = \frac{1}{2h}\left(\lambda - \frac{1}{\lambda}\right)$. Explicitly,

$$\begin{aligned} \hat{u} &= \tfrac{1}{\bar{u}\partial^u(e^{i\omega})}\left(\bar{f}_1 - \tfrac{\partial^c(e^{i\omega})}{\rho}\left(\tfrac{-\rho c^2 \partial^c(e^{i\omega})\bar{f}_1 + \bar{u}\partial^u(e^{i\omega})\bar{f}_2}{\mathcal{F}^h(e^{i\omega})}\right)\right), \\ \hat{\psi} &= \tfrac{\mathcal{D}^h(e^{i\omega})}{\bar{u}\partial^u(e^{i\omega})}\left(\tfrac{-\rho c^2 \partial^c(e^{i\omega})\bar{f}_1 + \bar{u}\partial^u(e^{i\omega})\bar{f}_2}{\mathcal{F}^h(e^{i\omega})}\right), \\ \hat{p} &= \tfrac{-\rho c^2 \partial^c(e^{i\omega})\bar{f}_1 + \bar{u}\partial^u(e^{i\omega})\bar{f}_2}{\mathcal{F}^h(e^{i\omega})}. \end{aligned} \tag{4.9}$$

Recall, that $\mathcal{D}^h(\lambda) = \mathcal{F}^h(\lambda) - \left(\bar{u}^2\partial^u(\lambda)\partial^d(\lambda) - c^2(\partial^c(\lambda))^2\right)$, and $\mathcal{F}^h(\lambda)$ is a generalized symbol of the desired discrete full-potential operator. The choice of the exact solution (4.1) as a Fourier mode guarantees that $\mathbf{q}^h_{\rm par}$ is a second-order accurate approximation to $\mathbf{q}^h_{\rm exact}$. The solution (4.6), (4.9) satisfies the discrete equation (4.3) but not the discrete boundary conditions.

The general solution of the homogeneous system of equations (3.6) is a linear combination of characteristic solutions $\mathbf{z}_k$ in the form $\mathbf{z}_k(j) = \mathbf{v}_k \lambda_k^j$

$$\mathbf{q}^h_{\rm hom} \equiv \begin{pmatrix} u^h_{\rm hom} \\ \psi^h_{\rm hom} \\ p^h_{\rm hom} \end{pmatrix} = \sum_k c_k \mathbf{z}_k = \sum_k c_k \mathbf{v}_k \lambda_k^j, \tag{4.10}$$

where $\mathbf{z}_k$ are linearly independent solutions of $\mathbf{L^h}\mathbf{q}^h = 0$ corresponding to the roots λ_k of the characteristic equation

$$\det \mathbf{L^h}(\lambda) \equiv \bar{u}\partial^u(\lambda)\mathcal{F}^h(\lambda) = 0. \tag{4.11}$$

The general solution of the discrete equations (4.3) is

$$\mathbf{q}^h \equiv \begin{pmatrix} u^h \\ \psi^h \\ p^h \end{pmatrix} = \mathbf{q}^h_{\rm hom} + \mathbf{q}^h_{\rm par} = \sum_k c_k \mathbf{z}_k + \begin{pmatrix} \hat{u} \\ \hat{\psi} \\ \hat{p} \end{pmatrix} e^{i\omega j}, \tag{4.12}$$

where c_k are chosen to satisfy boundary conditions. For second-order accuracy, $\mathbf{q}^h_{\rm hom}$ must be $O(h^2)$-small. The discretization error function is defined as

$$\mathbf{q}^h - \mathbf{q}^h_{\rm exact}. \tag{4.13}$$

5. Analysis of Boundary Conditions. Well-posedness of a linear discrete problem is equivalent to solvability and solution uniqueness of the linear system of equations obtained by substituting the general solution, $\mathbf{q}^h$, into the equations corresponding to (physical and numerical-closure) boundary conditions. The unknowns in the linear system are the coefficients c_k. This condition immediately implies that the total number of boundary-condition equations should be the same as the number of linearly independent characteristic solutions, z_k. Overspecified boundary conditions seemingly violate this condition but often provide a well-posed discrete problem. However, as we will show later in Section 6, the set of overspecified boundary conditions is equivalent to another set that exactly satisfies the relation between the number of boundary conditions and the number of linearly independent characteristic solutions.

The number of linearly independent characteristic solutions (and therefore the number of free parameters c_k) is defined by the length in mesh sizes (number of nodes minus 1) of the determinant operator stencil. The stencil should be considered as a "maximal-length footprint" before any possible cancellations occur. The stencil actually provides a more detailed information: the number of nodes left (right) of the center indicates the total number of required (physical and numerical-closure) boundary conditions at the left (right) boundary. Further specification, including a separate count for physical and numerical-closure equations, can be obtained from analysis of the set of linearly independent characteristic solutions. For I-stable discretizations, the characteristic solutions corresponding to $|\lambda_k| = 1$ relate to the solutions of the differential equations and are associated with physical boundary conditions. The characteristic solutions corresponding to $|\lambda_k| < 1$ relate to the discrete solutions decreasing exponentially fast as functions of the distance in mesh sizes from the left boundary. These characteristic solutions are associated with (define the number of) numerical-closure equations at the left (inflow) boundary. Analogously, the characteristic solutions corresponding to $|\lambda_k| > 1$ relate to the discrete solutions fast decreasing as functions of the distance in mesh sizes from the right boundary and define the number of numerical-closure equations at the right (outflow) boundary. Furthermore, analysis of the boundary-condition-sensitivity (**BCS**) matrix relating the coefficients c_k with the boundary conditions gives a precise indication of B-stability and accuracy order of the corresponding solution. For B-stability, all the coefficients of **BCS**matrix must be bounded as h tends to zero. The accuracy order can be estimated from the amplitude of $\mathbf{q}^h_{\text{hom}}$.

The following example illustrates the **BCS**matrix analysis in application to a particular second-order accurate discretization of a system of two simple uncoupled equations. The **BCS**matrix analysis of the discrete problem reveals that for achieving second-order accuracy, some of the numerical-closure equations must be second-order accurate. This fact contradicts a common belief that one can keep the target accuracy order by approximating numerical-closure equations with one-order lower accuracy than the interior equations.

The target differential equations are

$$\begin{aligned} \partial_x v &= g^1, \\ \partial_x w &= g^2. \end{aligned} \tag{5.1}$$

Let the exact solution of the differential problem defined on the interval $x \in [0,1]$ be

$$\begin{pmatrix} v(x) \\ w(x) \end{pmatrix} = \begin{pmatrix} C_v \\ C_w \end{pmatrix} e^{i\alpha x}, \tag{5.2}$$

then

$$\begin{pmatrix} g^1(x) \\ g^2(x) \end{pmatrix} = \begin{pmatrix} C_v \\ C_w \end{pmatrix} i\alpha e^{i\alpha x}, \tag{5.3}$$

and the boundary conditions associated with (5.1) are

$$\begin{aligned} v(0) &= C_v, \\ w(0) &= C_w. \end{aligned} \tag{5.4}$$

The second-order accurate discrete scheme employed for (5.1) on a uniform grid with mesh size h is defined as

$$\begin{pmatrix} \partial^u & 0 \\ h^2\partial^{(\mathrm{iv})} & \partial^u \end{pmatrix} \begin{pmatrix} v_j^h \\ w_j^h \end{pmatrix} = \begin{pmatrix} g^1(jh) \\ g^2(jh) \end{pmatrix}, \tag{5.5}$$

where v_j^h and w_j^h $(j = 0, 1, \ldots, N, N = 1/h)$ are discrete functions representing the continuous solutions $v(x)$ and $w(x)$, and

$$\begin{aligned} \partial^u v_j^h &\equiv \tfrac{1}{h}\Big(\tfrac{3}{2}v_j^h - 2v_{j-1}^h + \tfrac{1}{2}v_{j-2}^h\Big), \\ \partial^u w_j^h &\equiv \tfrac{1}{h}\Big(\tfrac{3}{2}w_j^h - 2w_{j-1}^h + \tfrac{1}{2}w_{j-2}^h\Big), \\ \partial^{(\mathrm{iv})} v_j^h &\equiv \tfrac{1}{h^4}\Big(v_{j+2}^h - 4v_{j+1}^h + 6v_j^h - 4v_{j-1}^h + v_{j-2}^h\Big). \end{aligned} \tag{5.6}$$

The determinant of the matrix in (5.5) is a seven-point discrete operator with the maximal-length footprint stencil

$$\frac{1}{4h^2}\begin{bmatrix} 1 & -8 & 22 & -24 & \underline{9} & 0 & 0 \end{bmatrix} \tag{5.7}$$

centered at the underlined position. Thus, a set of boundary conditions for the discrete equations (5.5) must include four boundary conditions at the left boundary and two boundary conditions at the right boundary. The characteristic equation for (5.5) is

$$\tfrac{1}{\lambda^4} - 8\tfrac{1}{\lambda^3} + 22\tfrac{1}{\lambda^2} - 24\tfrac{1}{\lambda} + 9 + 0\lambda + 0\lambda^2 = 0. \tag{5.8}$$

Two zero coefficients before the highest powers of λ imply that there are two infinity roots of the characteristic polynomial. Equation (5.8) has total six roots $\lambda_{1,2} = 1, \lambda_{3,4} = \frac{1}{3}$, and $\lambda_{5,6} = \infty$. A set of linearly independent characteristic solutions $\mathbf{z}_k(j) = \mathbf{v}_k\lambda_k^j$ is given by

$$\mathbf{v}_1 = \begin{pmatrix} 1 \\ 0 \end{pmatrix} \quad \text{and} \quad \mathbf{v}_2 = \begin{pmatrix} 0 \\ 1 \end{pmatrix} \tag{5.9}$$

corresponding to $\lambda_{1,2} = 1$,

$$\mathbf{v}_3 = \begin{pmatrix} 0 \\ 1 \end{pmatrix} \quad \text{and} \quad \mathbf{v}_4 = \begin{pmatrix} -h\frac{\frac{2}{\lambda_4} - \frac{1}{\lambda_4^2}}{\lambda_4^2 - 4\lambda_4 + 6 - 4\frac{1}{\lambda_4} + \frac{1}{\lambda_4^2}} \\ j \end{pmatrix} = \begin{pmatrix} \frac{27}{16}h \\ j \end{pmatrix} \tag{5.10}$$

corresponding to $\lambda_{3,4} = \frac{1}{3}$. Characteristic solutions corresponding to λ_5 and λ_6 exhibit nonzero values only near the right boundary and are zero in the interior and at the left boundary. Two characteristic solutions corresponding to $\lambda_{5,6} = \infty$ are

$$\mathbf{z}_5 = \begin{pmatrix} 0 \\ \delta_{N-1,j} \end{pmatrix} \quad \text{and} \quad \mathbf{z}_6 = \begin{pmatrix} 0 \\ \delta_{N,j} \end{pmatrix}, \qquad \delta_{k,j} = \begin{cases} 0, & \text{if} \quad k \neq j, \\ 1, & \text{if} \quad k = j. \end{cases} \tag{5.11}$$

The characteristic solutions, $\mathbf{z}_k$, are normalized to satisfy $\max_j |\mathbf{z}_k(j)| = O(1)$. Two sets of boundary conditions for the discrete system (5.5) are tested:

Set (A):

$$
\begin{array}{lll}
\text{(i)} & v_0^h & = C_v, \\
\text{(ii)} & w_0^h & = C_w, \\
\text{(iii)}_\text{a} & \frac{1}{h}\left(v_1^h - v_0^h\right) & = g^1(h), \\
\text{(iv)} & \frac{1}{h}\left(w_1^h - w_0^h\right) & = g^2(h), \\
\text{(v)} & \frac{1}{h}\left(\frac{3}{2}w_{N-1}^h - 2w_{N-2}^h + \frac{1}{2}w_{N-3}^h\right) & = g^2(1-h), \\
\text{(vi)} & \frac{1}{h}\left(\frac{3}{2}w_N^h - 2w_{N-1}^h + \frac{1}{2}w_{N-2}^h\right) & = g^2(1)
\end{array}
\tag{5.12}
$$

Set (B) is similar to Set (A) with condition $(\text{iii})_\text{a}$ replaced with a central second-order accurate approximation

$$
(\text{iii})_\text{b} \quad \frac{1}{2h}\left(v_2^h - v_0^h\right) = g^1(h). \tag{5.13}
$$

The equations (i) and (ii) correspond to the physical boundary conditions, all other equations are numerical-closure equations. The only difference between sets (A) and (B) is the approximation order of the numerical-closure equation (iii) at $j = 1$. The general solution can be represented in a form similar to (4.12)

$$
\begin{pmatrix} v_j^h \\ w_j^h \end{pmatrix} = \sum_{k=1}^{6} c_k \mathbf{z}_k + \begin{pmatrix} \hat{v} \\ \hat{w} \end{pmatrix} e^{i\omega j}, \tag{5.14}
$$

where $\omega = \alpha h$,

$$
\begin{array}{ll}
\hat{v} = & i\alpha C_v \frac{1}{\partial^u(e^{i\omega})}, \\
\hat{w} = & i\alpha\left(C_w - C_v \frac{h^2 \partial^{(\text{iv})}(e^{i\omega})}{\partial^u(e^{i\omega})}\right) \frac{1}{\partial^u(e^{i\omega})},
\end{array}
\tag{5.15}
$$

and the generalized symbols of discrete first and fourth derivatives are

$$
\begin{array}{ll}
\partial^u(\lambda) = & \frac{1}{h}\left(\frac{3}{2} - 2\frac{1}{\lambda} + \frac{1}{2}\frac{1}{\lambda^2}\right), \\
\partial^{(\text{iv})}(\lambda) = & \frac{1}{h^4}\left(\frac{1}{\lambda^2} - 4\frac{1}{\lambda} + 6 - 4\lambda + \lambda^2\right).
\end{array}
\tag{5.16}
$$

The exact solution (5.2) has been chosen so that the particular solution, $(\hat{v}, \hat{w})^T e^{i\omega j}$, of the problem (5.5) is a second-order accurate approximation to $(v, w)^T$. Thus, to keep second-order accuracy, the part of (5.14) related to the homogeneous solution $(\sum_{k=1}^{6} c_k \mathbf{z}_k)$ must be $O(h^2)$. Since $\max_j |\mathbf{z}_k(j)| = O(1), k = 1, \cdots, 6$, the amplitude of the homogeneous solution is determined by the coefficients $\mathbf{c} = (c_1, c_2, \ldots, c_6)^T$.

The coefficients $\mathbf{c}$ relate to the boundary conditions through matrix $\mathbf{B}$.

$$
\mathbf{B}\,\mathbf{c} + \tilde{\mathbf{d}} = 0, \tag{5.17}
$$

where vector $\tilde{\mathbf{d}} = (\tilde{d}_1, \tilde{d}_2, \ldots, \tilde{d}_6)^T$ is the vector of items independent of c_k obtained from substitution of the general solution (5.14) to a particular set of boundary conditions. For set (A),

$$
\mathbf{B} = \begin{pmatrix}
1 & 0 & 0 & \frac{27}{16}h & 0 & 0 \\
0 & 1 & 1 & 0 & 0 & 0 \\
0 & 0 & 0 & -\frac{9}{8} & 0 & 0 \\
0 & 0 & -\frac{2}{3h} & \frac{1}{3h} & 0 & 0 \\
0 & 0 & 0 & -\frac{1}{3^{N-3}h} & \frac{3}{2h} & 0 \\
0 & 0 & 0 & -\frac{1}{3^{N-2}h} & -\frac{2}{h} & \frac{3}{2h}
\end{pmatrix}
\tag{5.18}
$$

and

$$\tilde{\mathbf{d}} = -\begin{pmatrix} C_v - \hat{v} \\ C_w - \hat{w} \\ g^1(h) - \hat{v}\frac{1-e^{-i\omega}}{h}e^{i\omega} \\ g^2(h) - \hat{w}\frac{1-e^{-i\omega}}{h}e^{i\omega} \\ g^2(1-h) - \hat{w}\frac{\frac{3}{2}-2e^{-i\omega}+\frac{1}{2}e^{-i2\omega}}{h}e^{i(N-1)\omega} \\ g^2(1) - \hat{w}\frac{\frac{3}{2}-2e^{-i\omega}+\frac{1}{2}e^{-i2\omega}}{h}e^{i(N)\omega} \end{pmatrix}. \tag{5.19}$$

The main indication that the chosen set of boundary conditions is legitimate is the fact that matrix $\mathbf{B}$ is invertible, i.e., $\det \mathbf{B} \neq 0$, and the discrete problem (5.5), (5.12) is well posed. Thus, the well-posedness requirement (2) to practical sets of boundary conditions (Section 1) is satisfied. From (5.17),

$$\mathbf{c} = -\mathbf{B}^{-1}\,\tilde{\mathbf{d}}. \tag{5.20}$$

Normalization of $\tilde{\mathbf{d}}$ entries facilitating the analysis of B-stability leads to

$$\mathbf{d} = \mathbf{D}\,\tilde{\mathbf{d}}, \tag{5.21}$$

where entries of the diagonal matrix $\mathbf{D}$ are chosen so that the boundary data appear in $\mathbf{d}$ with $O(1)$ coefficients. For many practical boundary-condition sets, the coefficients of the quantities of interest are already $O(1)$ in $\tilde{\mathbf{d}}$, and therefore the vectors $\mathbf{d}$ and $\tilde{\mathbf{d}}$ are identical ($\mathbf{D}$ is the unity matrix), however, the overspecified boundary conditions result in distinguished $\mathbf{d}$ and $\tilde{\mathbf{d}}$. The **BCS**matrix is defined as

$$\mathbf{BCS} = \mathbf{B}^{-1}\,\mathbf{D}^{-1}. \tag{5.22}$$

In general, a discrete problem is B-stable in any norm (according to Definition of B-stability in Section 1), if all the entries of the **BCS**matrix remain bounded as h tends to zero. Even with some unbounded **BCS**matrix entries (tending to infinity as h tends to zero), the problem can still be B-stable in some common integral norms, such as L_2 or L_1. This is the case when the unbounded entries are located in the rows of the **BCS**matrix corresponding to non-physical characteristic solutions with λ_k separated from 1. Furthermore, given the accuracy of boundary-condition approximations, the **BCS**matrix predicts the size of the coefficients c_k and, hence, the approximation accuracy of the discrete solution. Actually, for B-stability and accuracy predictions, one does not need to compute the exact inverse $\mathbf{B}^{-1}$; it is enough to estimate the asymptotic behavior of the entries of the **BCS**matrix as functions of h.

In our example (set (A)),

$$\mathbf{BCS} = \begin{pmatrix} O(1) & 0 & O(h) & 0 & 0 & 0 \\ 0 & O(1) & O(1) & O(h) & 0 & 0 \\ 0 & 0 & O(1) & O(h) & 0 & 0 \\ 0 & 0 & O(1) & 0 & 0 & 0 \\ 0 & 0 & o(h) & 0 & O(h) & 0 \\ 0 & 0 & o(h) & 0 & O(h) & O(h) \end{pmatrix}, \tag{5.23}$$

where $o(h)$ is an exponentially small function of h (e.g., $O\left(3^{-\frac{1}{h}}\right)$). The discrete problem (5.5), (5.12) is B-stable because the **BCS**matrix (5.23) does not contain any entry growing as h tends to zero. The global accuracy mainly depends on c_1 and c_2 because $\lambda_{1,2} = 1$, and all other λ_k are well separated from zero. From

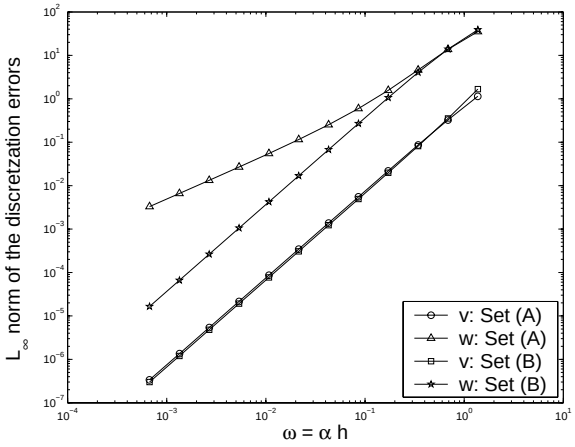

FIG. 5.1. *Discretization errors in v and w.*

the first row of (5.23), the accuracy of computing the coefficient c_1 depends on the approximation of the boundary conditions (i) and (iii). If boundary condition (i) is at least second-order accurate and boundary condition (iii) is at least first-order accurate (that is the case in both sets (A) and (B)) then the coefficient c_1 is computed with at least second-order accuracy. Similarly, the accuracy of computing the coefficient c_2 depends on the approximation of the boundary conditions (ii), (iii), and (iv). From the second row of (5.23), one can conclude that the accuracy order in computing c_2 usually cannot be better than the approximation order for the boundary condition (iii). In set (A), the boundary condition $(\text{iii})_\text{a}$ is a first-order accurate approximation to the first equation of (5.5). Therefore, the third element in $\mathbf{d}$ is $O(h)$-small. Generally, when a set of boundary condition is changed, the **BCS**matrix should be recomputed. However, if two sets differ only in approximations to the same equations, the **BCS**matrix remains unchanged. In set (B), the boundary condition $(\text{iii})_\text{b}$ is a second-order accurate approximation to the first equation of (5.5), and $d_3 = O(h^2)$. Thus, one can expect that, with set (A) of boundary conditions, function w is approximated with first-order accuracy, and, with set (B), w is approximated with second-order accuracy. Function v is approximated with second-order accuracy in any case. Figure 5.1 confirms this prediction. On the figure, the L_∞-norm of discretization errors computed for $C_v = 1, C_w = 2, \alpha = 7\pi$ on a sequence of grids with $h = 2^{-4}, 2^{-5}, \cdots, 2^{-15}$ is shown.

6. Boundary Conditions for Factorizable Discretizations. In this section, the boundary conditions for two versions of the discrete system (4.3) are considered. The versions differ in the desired form for the discrete full-potential operator and, therefore, in the discrete representation for the operator $\mathcal{D}^h$. In the first version, the discrete full-potential operator employs a five-point discrete operator $\partial^h_{xx} = \partial^u \partial^d$ that is a composition of second-order accurate upwind and downwind difference approximations for the first derivative.

$$\begin{aligned} \partial^h_{xx} p^h_j &= \tfrac{1}{h^2}\left(-\tfrac{3}{4}p^h_{j+2} + 4p^h_{j+1} - \tfrac{13}{2}p^h_j + 4p^h_{j-1} - \tfrac{3}{4}p^h_{j-2}\right), \\ \mathcal{D}^h p^h_j &= \tfrac{c^2}{h^2}\left(p^h_{j+2} - 4p^h_{j+1} + 6p^h_j - 4p^h_{j-1} + p^h_{j-2}\right). \end{aligned} \tag{6.1}$$

The discrete operator ∂^h_{xx} used in the second version is a three-point central approximation as

$$\begin{aligned} \partial^h_{xx} p^h_j &= \tfrac{1}{h^2}\left(p^h_{j+1} - 2p^h_j + p^h_{j-1}\right), \\ \mathcal{D}^h p^h_j &= \tfrac{3\bar{u}^2 + c^2}{4h^2}\left(p^h_{j+2} - 4p^h_{j+1} + 6p^h_j - 4p^h_{j-1} + p^h_{j-2}\right). \end{aligned} \tag{6.2}$$

All other operators used in the versions of (4.3) are the same:

$$
\begin{array}{ll}
\partial^u u_j^h = & \frac{1}{h}\left(\frac{3}{2}u_j^h - 2u_{j-1}^h + \frac{1}{2}u_{j-2}^h\right), \\
\partial^c p_j^h = & \frac{1}{h}\left(\frac{1}{2}p_{j+1}^h - \frac{1}{2}p_{j-1}^h\right), \\
\partial^u \psi_j^h = & \frac{1}{h}\left(\frac{3}{2}\psi_j^h - 2\psi_{j-1}^h + \frac{1}{2}\psi_{j-2}^h\right), \\
\partial^c u_j^h = & \frac{1}{h}\left(\frac{1}{2}u_{j+1}^h - \frac{1}{2}u_{j-1}^h\right), \\
\partial^d p_j^h = & \frac{1}{h}\left(-\frac{3}{2}p_j^h + 2p_{j+1}^h - \frac{1}{2}p_{j+2}^h\right),
\end{array}
\tag{6.3}
$$

For both the versions, the determinant is a seven-point upwind-biased operator implying that boundary conditions must contain four boundary conditions specified at the inflow boundary and two boundary conditions specified at the outflow boundary. Two physical boundary conditions (4.5) are defined at the inflow boundary, and one physical boundary condition is defined at the outflow boundary. Thus, two inflow and one outflow numerical-closure equations are required. In examples below, the following sets of boundary conditions are analyzed:

(A) *Overspecified boundary conditions*, where values of $u_{-1}^h, u_0^h, u_N^h, u_{N+1}^h, p_{-1}^h, p_0^h, p_N^h, p_{N+1}^h$, are specified from the exact continuous solution (4.1), and $\psi_{-1}^h = \psi_0^h = \psi_N^h = \psi_{N+1}^h = 0$. The total number of specified values is twelve, but it can be reduced to the following six boundary conditions:

$$
\begin{array}{lll}
\text{(i)} & u_0^h & = C_u, \\
\text{(ii)} & \bar{u}\partial^u u_1^h + \frac{1}{\rho}\partial^c p_1^h & = f_1(h), \\
\text{(iii)} & \bar{u}\partial^u \psi_1^h - \mathcal{D}^h p_1^h & = 0, \\
\text{(iv)} & \bar{u}\partial^u \psi_2^h - \mathcal{D}^h p_2^h & = 0, \\
\text{(v)} & \rho c^2 \partial^c u_{N-1}^h + \psi_{N-1}^h + \bar{u}\partial^d p_{N-1}^h & = f_2(1-h), \\
\text{(vi)} & p_N^h & = C_p e^{i\alpha}.
\end{array}
\tag{6.4}
$$

The equations (ii), (iii), (iv), and (v), used in the boundary-condition formulation are modified from the interior equations because all the values with indexes -1, 0, N, $N+1$ required for computation are taken from the overspecified boundary conditions and cannot be computed (except u_0^h and p_N^h) from the general solution representation (4.12). Note also, that for computation of (v) one should use the value of ψ_{N-1}^h that, in turn, computed from a modified equation $\bar{u}\partial^u \psi_{N-1}^h - \mathcal{D}^h p_{N-1}^h = 0$.

(B) *Practical boundary conditions.* Sets of practical boundary conditions that contain only physically available boundary data are described. The sets differ in the way they reconstruct value u_{-1}^h.

$$
\begin{array}{lll}
\text{(i)} & u_0^h & = C_u, \\
\text{(ii)} & \psi_0^h & = 0, \\
\text{(iii)} & \bar{u}\frac{1}{h}\left(\psi_1^h - \psi_0^h\right) & = 0, \\
\text{(iv)}_\text{b} & \frac{1}{h^3}\left(u_2^h - 3u_1^h + 3u_0^h - u_{-1}^h\right) & = 0, \\
\text{(v)} & \frac{1}{h^3}\left(p_{N+1}^h - 3p_N^h + 3p_{N-1}^h - p_{N-2}^h\right) & = 0, \\
\text{(vi)} & p_N^h & = C_p e^{i\alpha}.
\end{array}
\tag{6.5}
$$

The conditions (ii) and (iii) imply $\psi_1^h = 0$. One can interpret the boundary conditions (iv)_b and (v) as a second-order extrapolation from the interior for the value of u_{-1}^h and p_{N+1}^h. The conditions (iv)_b and (v) are numerical-closure boundary conditions because they relate outside values of functions u_j^h and p_j^h with inner values. These two conditions are equivalent to simultaneous modification of equations $r_1(\mathbf{q^h})_1 = f_1(h), r_3(\mathbf{q^h})_0 = f_2(0), r_1(\mathbf{q^h})_N = f_1(1)$ and $r_3(\mathbf{q^h})_{N-1} = f_2(1-h)$. (See (3.6) for definitions of $r_k(\mathbf{q^h})_j$.)

(C) *Practical boundary conditions.* This and two other tested sets of boundary conditions are similar to set (B). The only difference is the condition $(\mathrm{iv})_\mathrm{b}$ is replaced with

$$(\mathrm{iv})_\mathrm{c} \quad \tfrac{1}{h^3}\left(p_3^h - 3p_2^h + 3p_1^h - p_0^h\right) \quad = 0, \tag{6.6}$$

The condition $(\mathrm{iv})_\mathrm{c}$ may be regarded as a second-order extrapolation of the value p_0^h from the interior. The interior equation $r_3(\mathbf{q^h})_0 = f_2(0)$ is used to compute u_{-1}^h. The condition $(\mathrm{iv})_\mathrm{c}$ is equivalent to simultaneous modification of equations $r_1(\mathbf{q^h})_1 = f_1(h)$ and $r_2(\mathbf{q^h})_2 = 0$.

(D) *Practical boundary conditions.*

$$(\mathrm{iv})_\mathrm{d} \quad \tfrac{\bar{u}^2-c^2}{h}\left(\tfrac{1}{2}u_1^h - \tfrac{1}{2}u_{-1}^h\right) \quad = \bar{u}f_1(0) - \tfrac{1}{\rho}f_2(0), \tag{6.7}$$

The condition $(\mathrm{iv})_\mathrm{d}$ reconstructs u_{-1}^h from a second-order accurate central discrete approximation to the equation $(\bar{u}^2 - c^2)\partial_x u = \bar{u}f_1 - \frac{1}{\rho}f_2$ defined at the inflow boundary. The equation is derived by manipulating the differential equations from (2.5). This numerical-closure boundary condition is equivalent to simultaneous modification of equations $r_1(\mathbf{q^h})_1 = f_1(h)$ and $r_3(\mathbf{q^h})_0 = f_2(0)$.

(E) *Practical boundary conditions.*

$$(\mathrm{iv})_\mathrm{e} \quad \tfrac{\bar{u}}{h}\left(u_1^h - u_0^h\right) + \tfrac{1}{\rho h}\left(\tfrac{1}{2}p_2^h - \tfrac{1}{2}p_0^h\right) \quad = f_1(h), \tag{6.8}$$

The condition $(\mathrm{iv})_\mathrm{e}$ is shown to illustrate the importance of second-order accuracy in approximating the first and the third equations in (4.3) at the inflow boundary. Simultaneously with $(\mathrm{iv})_\mathrm{e}$, the interior second-order accurate equation $r_1(\mathbf{q^h})_1 = f_1(h)$ is used to recover u_{-1}^h.

6.1. Factorizable Scheme #1: 5-point Full-Potential Operator. Let ∂^u and ∂^d be second-order upwind and downwind discrete operators, respectively, ∂^c is the second-order central discretization, and $\mathcal{F}^h = (\bar{u}^2 - c^2)\partial^u\partial^d$. The generalized symbols are

$$\begin{aligned}
\partial^u(\lambda) &= \tfrac{1}{h}\left(\tfrac{3}{2} - 2\tfrac{1}{\lambda} + \tfrac{1}{2}\tfrac{1}{\lambda^2}\right), \\
\partial^d(\lambda) &= \tfrac{1}{h}\left(-\tfrac{3}{2} + 2\lambda - \tfrac{1}{2}\lambda^2\right), \\
\partial^c(\lambda) &= \tfrac{1}{h}\left(-\tfrac{1}{2}\tfrac{1}{\lambda} + \tfrac{1}{2}\lambda\right), \\
\mathcal{F}^h(\lambda) &= (\bar{u}^2 - c^2)\partial^u(\lambda)\partial^d(\lambda), \\
\mathcal{D}^h(\lambda) &= c^2\Big((\partial^c(\lambda))^2 - \partial^u(\lambda)\partial^d(\lambda)\Big) = \tfrac{c^2}{h^2}\left(\tfrac{1}{\lambda^2} - 4\tfrac{1}{\lambda} + 6 - 4\lambda + \lambda^2\right).
\end{aligned} \tag{6.9}$$

A particular solution of the nonhomogeneous problem is found by substitution of the generalized symbols to (4.9). The characteristic equation,

$$\Big(\partial^u(\lambda)\Big)^2\partial^d(\lambda) = 0, \tag{6.10}$$

has six roots $\lambda_{1,2,3} = 1$, $\lambda_{4,5} = \frac{1}{3}$, and $\lambda_6 = 3$.

Before presenting the general solution, let us introduce some auxiliary symbol-like functions that are required for defining linearly independent characteristic solutions.

$$\begin{aligned}
\hat{\partial^u}(\lambda) &= \tfrac{1}{h}\left(2\tfrac{1}{\lambda} - \tfrac{1}{\lambda^2}\right), \\
\hat{\partial^c}(\lambda) &= \tfrac{1}{h}\left(\tfrac{1}{2}\tfrac{1}{\lambda} + \tfrac{1}{2}\lambda\right),
\end{aligned} \tag{6.11}$$

The six linearly independent characteristic solutions, $\mathbf{z}_k(j) = \mathbf{v}_k(j)\lambda_k^j$, are given by:

$$\mathbf{v}_1 = \begin{pmatrix} 1 \\ 0 \\ 0 \end{pmatrix}, \mathbf{v}_2 = \begin{pmatrix} 0 \\ 0 \\ 1 \end{pmatrix}, \text{ and } \mathbf{v}_3 = \begin{pmatrix} jh \\ \rho c^2 \left(\frac{\bar{u}^2}{c^2} - 1 \right) \\ -jh\rho\bar{u} \end{pmatrix} \tag{6.12}$$

corresponding to $\lambda_{1,2,3} = 1$,

$$\mathbf{v}_4 = \begin{pmatrix} h \\ -\rho c^2 h \partial^c(\lambda_4) \\ 0 \end{pmatrix} = \begin{pmatrix} h \\ \frac{4}{3}\rho c^2 \\ 0 \end{pmatrix}$$

and

$$\mathbf{v}_5 = \begin{pmatrix} jh \\ \rho c^2 h \left(\frac{\bar{u}^2}{c^2} \frac{\partial^d(\lambda_5)\hat{\partial}^u(\lambda_5)}{\partial^c(\lambda_5)} - \hat{\partial}^c(\lambda_5) - j\partial^c(\lambda_5) \right) \\ -h\rho\bar{u}\frac{\hat{\partial}^u(\lambda_5)}{\partial^c(\lambda_5)} \end{pmatrix} = \begin{pmatrix} jh \\ \rho c^2 \left(-2\frac{\bar{u}^2}{c^2} - \frac{5}{3} + j\frac{4}{3} \right) \\ -\frac{9}{4}h\rho\bar{u} \end{pmatrix} \tag{6.13}$$

corresponding to $\lambda_{4,5} = \frac{1}{3}$, and

$$\mathbf{v}_6 = (\lambda_6)^{-N} \begin{pmatrix} h \\ -\rho c^2 h \partial^c(\lambda_6) \\ -h\rho\bar{u}\frac{\partial^u(\lambda_6)}{\partial^c(\lambda_6)} \end{pmatrix} = (\lambda_6)^{-N} \begin{pmatrix} h \\ -\frac{4}{3}\rho c^2 \\ -h\frac{2}{3}\rho\bar{u} \end{pmatrix} \tag{6.14}$$

corresponding to $\lambda_6 = 3$. The characteristic solutions are normalized to satisfy $\max_j |\mathbf{z}_k(j)| = O(1)$ for h tending to zero.

For overspecified boundary conditions (set (A)),

$$\tilde{\mathbf{d}} = -\begin{pmatrix} \delta u_0^h \\ -\frac{\bar{u}}{2h}\delta u_{-1}^h + \frac{1}{2\rho h}\delta p_0^h \\ -\frac{\bar{u}}{2h}(-4\delta\psi_0^h + \delta\psi_{-1}^h) + \frac{c^2}{h^2}(-4\delta p_0^h + \delta p_{-1}^h) \\ -\frac{\bar{u}}{2h}\delta\psi_0^h + \frac{c^2}{h^2}\delta p_0^h \\ -\frac{\rho c^2}{2h}\delta u_N^h + \frac{3\bar{u}^2 - 4c^2}{6\bar{u}h}\delta p_{N+1}^h \\ \delta p_N^h \end{pmatrix}, \quad \mathbf{D} = \begin{pmatrix} 1 & 0 & 0 & 0 & 0 & 0 \\ 0 & h & 0 & 0 & 0 & 0 \\ 0 & 0 & h^2 & 0 & 0 & 0 \\ 0 & 0 & 0 & h^2 & 0 & 0 \\ 0 & 0 & 0 & 0 & h & 0 \\ 0 & 0 & 0 & 0 & 0 & 1 \end{pmatrix} \tag{6.15}$$

$$\mathbf{d} = \mathbf{D}\,\tilde{\mathbf{d}} = -\begin{pmatrix} \delta u_0^h \\ -\frac{\bar{u}}{2}\delta u_{-1}^h + \frac{1}{2\rho}\delta p_0^h \\ -\frac{\bar{u}h}{2}(-4\delta\psi_0^h + \delta\psi_{-1}^h) + c^2(-4\delta p_0^h + \delta p_{-1}^h) \\ -\frac{\bar{u}h}{2}\delta\psi_0^h + c^2\delta p_0^h \\ -\frac{\rho c^2}{2}\delta u_N^h + \frac{3\bar{u}^2 - 4c^2}{6\bar{u}}\delta p_{N+1}^h \\ \delta p_N^h \end{pmatrix}, \tag{6.16}$$

and

$$\mathbf{BCS} = \begin{pmatrix} O(1) & O(1) & O(1) & O(1) & O(1) & O(h) \\ O(1) & O(1) & O(1) & O(1) & O(1) & O(h) \\ O(1) & O(1) & O(1) & O(1) & O(1) & O(1) \\ O(1/h) & O(1/h) & O(1/h) & O(1/h) & O(1/h) & O(1) \\ O(1/h) & O(1/h) & O(1/h) & O(1/h) & O(1/h) & O(1) \\ O(1/h) & O(1/h) & O(1/h) & O(1/h) & O(1/h) & O(1/h) \end{pmatrix}, \tag{6.17}$$

where $\delta\mathbf{q}_j^h = (\mathbf{q^h}_{\rm exact})_j - (\mathbf{q^h}_{\rm par})_j$, $\delta\mathbf{q}_j^h \equiv (\delta u_j^h, \delta\psi_j^h, \delta p_j^h)^T$. The solution of the discrete problem (4.3) with the overspecified boundary conditions is obviously B-unstable according to Definition of B-stability given in the introductory Section 1. Indeed, upon any fixed perturbation of the overspecified boundary conditions, the coefficients c_4, c_5, and c_6 grow with h tending to zero. However, there are two factors that allow considering this discrete scheme as satisfactory:

1) The unbounded entries of the **BCS**matrix affect only the coefficients of the "non-physical" characteristic solutions, (i.e., the characteristic solutions corresponding to λ_k with amplitudes separated from unity) and, therefore, decrease exponentially fast away from boundaries as functions of the mesh index. So the discrete solution remains bounded in any common integral norm (e.g., L_2-norm).
2) Within the "non-physical" characteristic solutions, only the amplitude of the auxiliary function ψ^h is unbounded because the entries of $\mathbf{v}_4, \mathbf{v}_5$, and $\mathbf{v}_6$ related to physical variables, u^h and p^h, are $O(h)$-small in comparison with the entries related to ψ^h.

Recall that the values of $\delta\mathbf{q}_j^h$ are $O(h^2)$-small. Accordingly, if the overspecified boundary conditions are copied precisely from the exact continuous solution (4.1), the discrete solution of (4.3) is second-order accurate for the physical variables, u^h and p^h, in any norm; the L_∞-norm of ψ^h converges to zero as $O(h)$, and ψ^h is $O(h^2)$-small in any common integral norm. We found experimentally, that with exact overspecification, only c_6 behaves as $O(h)$; coefficients c_4 and c_5 are still $O(h^2)$. This better-than-expected behavior for c_4 and c_5 is explained by cancellations in computation of $\mathbf{B}^{-1}\tilde{\mathbf{d}}$. Upon an arbitrary $O(h^2)$ perturbation of the overspecified data, all the three coefficients, c_4, c_5, and c_6, become $O(h)$.

Vectors $\mathbf{d}$ are very similar for the sets (B) through (E); the only difference is the fourth element, d_4. For set (B),

$$\mathbf{d} \equiv \begin{pmatrix} d_1 \\ d_2 \\ d_3 \\ d_4^{(B)} \\ d_5 \\ d_6 \end{pmatrix} = - \begin{pmatrix} C_u - \hat{u} \\ -\hat{\psi} \\ \bar{u}\hat{\psi}\frac{e^{i\omega}-1}{h} \\ -\hat{u}\frac{e^{i2\omega}-3e^{i\omega}+3-e^{-i\omega}}{h^3} \\ -\hat{p}\frac{e^{i(N+1)\omega}-3e^{iN\omega}+3e^{i(N-1)\omega}-e^{i(N-2)\omega}}{h^3} \\ (C_p - \hat{p})e^{iN\omega} \end{pmatrix}, \tag{6.18}$$

where $\hat{u}, \hat{\psi}$, and $\hat{p}$ are given in (4.9) with generalized symbols defined in (6.9).

$$\begin{aligned} d_4^{(C)} &= \hat{p}\frac{e^{i3\omega}-3e^{i2\omega}+3e^{i\omega}-1}{h^3}, \\ d_4^{(D)} &= -\frac{1}{c^2-\bar{u}^2}\left(\bar{u}f_1(0) - \frac{1}{\rho}f_2(0)\right) - \hat{u}\frac{e^{i\omega}-e^{-i\omega}}{2h}, \\ d_4^{(E)} &= f_1(h) - \left(\hat{u}\bar{u}\frac{e^{i\omega}-1}{h} + \hat{p}\frac{1}{\rho}\frac{e^{i\omega}-e^{-i\omega}}{2h}\right). \end{aligned} \tag{6.19}$$

The **BCS**matrices for tested practical boundary conditions fell in two categories: for sets (B) and (C),

$$\mathbf{BCS} = \begin{pmatrix} O(1) & 0 & O(h^2) & O(h^3) & o(h) & 0 \\ 0 & O(1) & O(h) & O(h^2) & O(h^3) & O(1) \\ 0 & O(1) & O(h) & O(h^2) & o(h) & 0 \\ 0 & 0 & O(h) & O(h^2) & o(h) & 0 \\ 0 & 0 & O(h) & O(h^2) & o(h) & 0 \\ 0 & 0 & o(h) & o(h) & O(h^2) & 0 \end{pmatrix}, \tag{6.20}$$

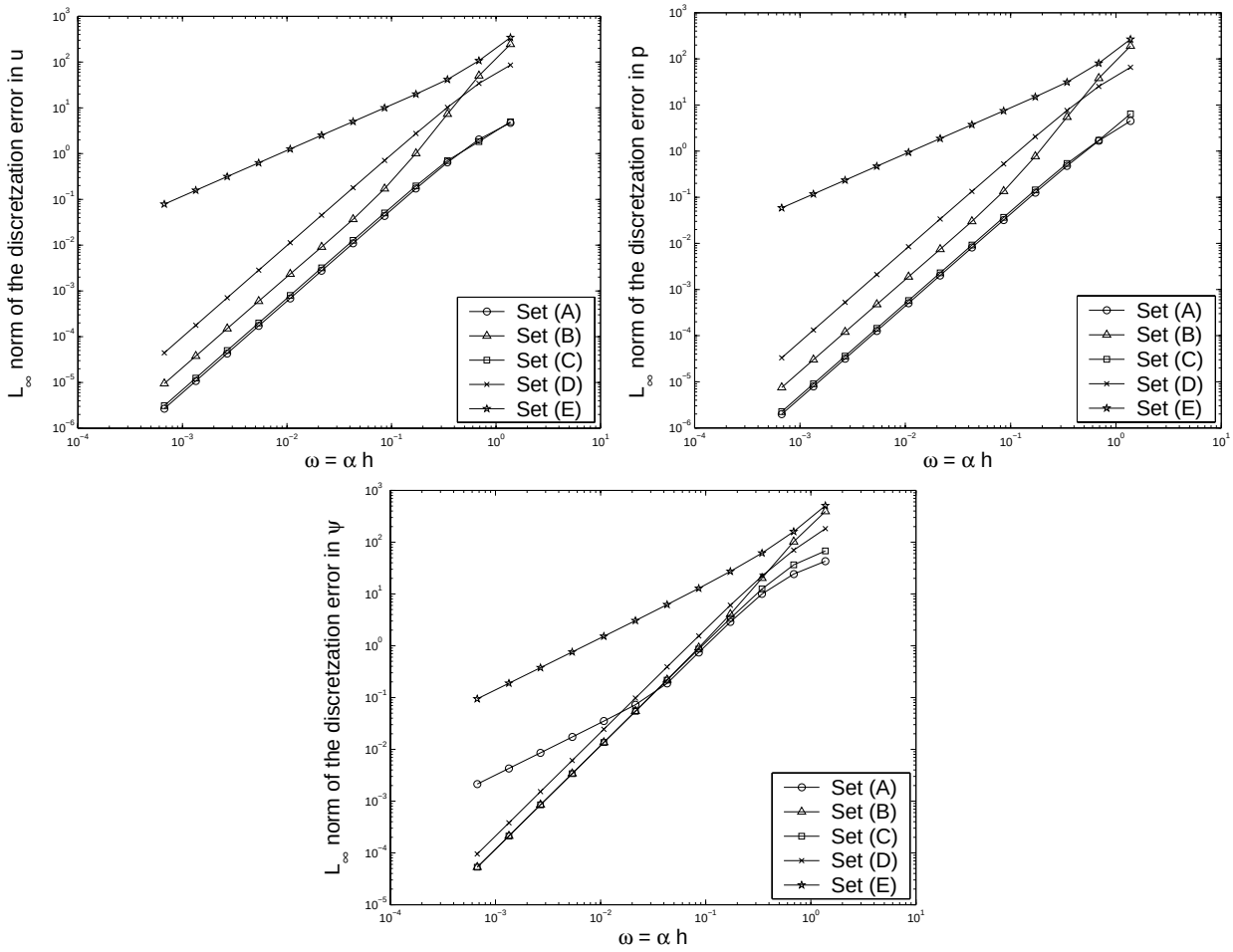

FIG. 6.1. *Scheme # 1: L_∞ norms of discretization errors in u, ψ, and p.*

and for sets (D) and (E),

$$\mathbf{BCS} = \begin{pmatrix} O(1) & O(h) & O(h^2) & O(h) & o(h) & 0 \\ 0 & O(1) & O(h) & O(1) & O(h^3) & O(1) \\ 0 & O(1) & O(h) & O(1) & o(h) & 0 \\ 0 & O(1) & O(h) & O(1) & o(h) & 0 \\ 0 & O(1) & O(h) & O(1) & o(h) & 0 \\ 0 & o(h) & o(h) & o(h) & O(h^2) & 0 \end{pmatrix}. \tag{6.21}$$

All the sets of practical boundary conditions provide solutions to the discrete problem (4.3) that are B-stable. Elements d_1, d_2, d_3, and d_6 are $O(h^2)$; d_5 is $O(1)$; $d_4^{(B)}$ and $d_4^{(C)}$ are $O(1)$; $d_4^{(D)}$ is $O(h^2)$; and $d_4^{(E)}$ is $O(h)$. Thus, for sets (B) through (D), the computation accuracy of coefficients c_k is at least second order, i.e., the Scheme # 1 is second-order accurate for all the (physical and auxiliary) variables in any norm. For set (E), first-order accuracy in computing c_2, c_3, c_4, and c_5 is expected. The impact of characteristic solutions $\mathbf{z}_2$ and $\mathbf{z}_3$ is global for all variables because $jh = O(1)$ for $j = O(N)$; therefore, the discretization errors in u^h, ψ^h, and p^h are $O(h)$ in any norm.

The results of numerical tests are shown in Figure 6.1. The tests have been performed for the non-

dimensional constant coefficients corresponding to a Mach number $M = 0.5$:

$$\begin{aligned} c &= \sqrt{\frac{1+\frac{\gamma-1}{2}}{1+M^2\frac{\gamma-1}{2}}}, \\ \rho &= c^{\frac{2}{\gamma-1}}, \\ \bar{u} &= cM, \end{aligned} \tag{6.22}$$

where $\gamma = 1.4$. The parameters of the exact continuous solution defined on the interval $x \in [0,1]$ have been chosen as $C_u = 1, C_p = 2$, and $\alpha = 7\pi$. The L_∞ norms of discretization errors have been measured for a sequence of uniform grids with $h = 2^{-4}, 2^{-5}, \ldots, 2^{-15}$. The results confirm exactly the predictions made by the **BCS**analysis. An important observation is that the choice of boundary conditions strongly affects the absolute value of the discretization errors. The gain from optimizing the set of boundary conditions may exceed an order of magnitude in solution accuracy on a given grid. Among the practical boundary conditions, set (C) seems to exhibit the minimum discretization errors for all the variables. For physical variables, the discretization errors with overspecified boundary conditions (set (A)) is minimal.

6.2. Factorizable Scheme #2: 3-point Full-Potential Operator. Let ∂^u and ∂^d remain the same as in Factorizable Scheme # 1, and $\mathcal{F}^h = (\bar{u}^2 - c^2)\partial^h_{xx}$, where ∂^h_{xx} is a three-point central second-order accurate approximation to the second derivative. The full-potential factor has formally a three-point stencil, however, its stencil should be considered as five-point long with zero coefficients (due to cancellations) at the outermost nodes. Therefore,

$$\mathcal{F}^h(\lambda) = \frac{\bar{u}^2 - c^2}{h^2}\left(\frac{0}{\lambda^2} + \frac{1}{\lambda} - 2 + \lambda + 0\lambda^2\right) \tag{6.23}$$

and

$$\mathcal{D}^h(\lambda) = \mathcal{F}^h(\lambda) - \left(\bar{u}^2\partial^u(\lambda)\partial^d(\lambda) - c^2(\partial^c(\lambda))^2\right) = \frac{3\bar{u}^2 + c^2}{4}\frac{1}{h^2}\left(\frac{1}{\lambda^2} - 4\frac{1}{\lambda} + 6 - 4\lambda + \lambda^2\right). \tag{6.24}$$

The characteristic equation

$$\partial^u(\lambda)\mathcal{F}^h(\lambda) = 0 \tag{6.25}$$

has six roots $\lambda_{1,2,3} = 1$, $\lambda_4 = \frac{1}{3}$, $\lambda_5 = 0$, and $\lambda_6 = \infty$. The same five sets of boundary conditions (sets (A) through (E)) are analyzed for Factorizable Scheme # 2. The scheme is characterized by presence of zero and infinite values of λ_k.

The solution representation as a linear combination of the functions $\mathbf{z}_k = \mathbf{v}_k\lambda_k^j$, is relevant only for finite, nonzero eigenvalues. For zero eigenvalue, the corresponding characteristic solutions are localized at the inflow boundary, i.e., they exhibit nonzero values at the inflow and are zero in the interior and at the outflow boundary. By analogy, characteristic solutions corresponding to infinite eigenvalue are localized at the outflow boundary, i.e., they are nonzero only at some locations in the vicinity of the outflow. Infinite values of λ_k have already appeared in the example in Section 5. However, in that example, the characteristic solutions related to infinite λ_k affected only one variable, w^h. In general, each characteristic solution may affect all the solution variables. In such a case, the nonzero values for primitive variables corresponding to a localized characteristic solution are usually featured at different j-locations. The exact placements of the nonzero entries are dictated by the three requirements:

(1) The corresponding matrix $\mathbf{B}$ relating the coefficients of characteristic solutions to the boundary conditions is invertible.

(2) The solution values outside of the limits defined by the placements are not needed for computing residuals of the interior equations.

(3) Multiplication of the localized characteristic solution by a constant does not change residuals in the interior equations.

Four linearly independent characteristic solutions corresponding to finite (nonzero) eigenvalues can be found in the usual form $\mathbf{z}_k(j) = \mathbf{v}_k \lambda_k^j$.

$$\mathbf{v}_1 = \begin{pmatrix} 1 \\ 0 \\ 0 \end{pmatrix}, \mathbf{v}_2 = \begin{pmatrix} 0 \\ 0 \\ 1 \end{pmatrix}, \text{ and } \mathbf{v}_3 = \begin{pmatrix} jh \\ \rho\left(\bar{u}^2 - c^2\right) \\ -jh\rho\bar{u} \end{pmatrix} \tag{6.26}$$

correspond to $\lambda_{1,2,3} = 1$, and

$$\mathbf{v}_4 = \begin{pmatrix} h \\ -h\rho c^2 \partial^c(\lambda_4) \\ 0 \end{pmatrix} = \begin{pmatrix} h \\ \frac{4}{3}\rho c^2 \\ 0 \end{pmatrix} \tag{6.27}$$

corresponds to $\lambda_4 = \frac{1}{3}$.

The placement of nonzero values of the localized characteristic solutions depends on the choice of boundary condition set. For overspecified boundary conditions (Set (A)), the characteristic solution, $\mathbf{z}_5$, localized at the inflow (i.e., corresponding to $\lambda_5 = 0$) is

$$\mathbf{z}_5(j) = \begin{pmatrix} h\,\delta_{0,j} \\ \rho\frac{3\bar{u}^2+c^2}{2}\,\delta_{1,j} \\ \rho\bar{u}h\,\delta_{1,j} \end{pmatrix} \tag{6.28}$$

and the characteristic solution, $\mathbf{z}_6$, localized at the outflow (i.e., corresponding to $\lambda_6 = \infty$) is

$$\mathbf{z}_6(j) = \begin{pmatrix} h\,\delta_{N-1,j} \\ -\rho\frac{3\bar{u}^2+c^2}{2}\,\delta_{N-2,j} \\ -3\rho\bar{u}h\,\delta_{N,j} \end{pmatrix} \tag{6.29}$$

For practical boundary conditions (sets (B) through (E)), the locations of nonzero entries are moving one mesh size outward, i.e.,

$$\mathbf{z}_5(j) = \begin{pmatrix} h\,\delta_{-1,j} \\ \rho\frac{3\bar{u}^2+c^2}{2}\,\delta_{0,j} \\ \rho\bar{u}h\,\delta_{0,j} \end{pmatrix} \tag{6.30}$$

and

$$\mathbf{z}_6(j) = \begin{pmatrix} h\,\delta_{N,j} \\ -\rho\frac{3\bar{u}^2+c^2}{2}\,\delta_{N-1,j} \\ -3\rho\bar{u}h\,\delta_{N+1,j} \end{pmatrix} \tag{6.31}$$

For overspecified boundary conditions (set (A)),

$$\mathbf{D} = \begin{pmatrix} 1 & 0 & 0 & 0 & 0 & 0 \\ 0 & h & 0 & 0 & 0 & 0 \\ 0 & 0 & h^2 & 0 & 0 & 0 \\ 0 & 0 & 0 & h^2 & 0 & 0 \\ 0 & 0 & 0 & 0 & h & 0 \\ 0 & 0 & 0 & 0 & 0 & 1 \end{pmatrix}, \quad \tilde{\mathbf{d}} = - \begin{pmatrix} \delta u_0^h \\ -\frac{\bar{u}}{2h}\delta u_{-1}^h + \frac{1}{2\rho h}\delta p_0^h \\ -\frac{\bar{u}}{2h}(-4\delta\psi_0^h + \delta\psi_{-1}^h) + \frac{3\bar{u}^2+c^2}{h^2}(-4\delta p_0^h + \delta p_{-1}^h) \\ -\frac{\bar{u}}{2h}\delta\psi_0^h + \frac{3\bar{u}^2+c^2}{h^2}\delta p_0^h \\ -\frac{\rho c^2}{2h}\delta u_N^h - \frac{9\bar{u}^2+4c^2}{6\bar{u}h}\delta p_{N+1}^h \\ \delta p_N^h \end{pmatrix}, \tag{6.32}$$

$$\mathbf{d} = \mathbf{D}\,\tilde{\mathbf{d}} = -\begin{pmatrix} \delta u_0^h \\ -\frac{\bar{u}}{2}\delta u_{-1}^h + \frac{1}{2\rho}\delta p_0^h \\ -\frac{\bar{u}h}{2}(-4\delta\psi_0^h + \delta\psi_{-1}^h) + (3\bar{u}^2 + c^2)(-4\delta p_0^h + \delta p_{-1}^h) \\ -\frac{\bar{u}h}{2}\delta\psi_0^h + (3\bar{u}^2 + c^2)\delta p_0^h \\ -\frac{\rho c^2}{2}\delta u_N^h - \frac{9\bar{u}^2+4c^2}{6\bar{u}}\delta p_{N+1}^h \\ \delta p_N^h \end{pmatrix}, \tag{6.33}$$

and

$$\mathbf{BCS} = \begin{pmatrix} O(1) & O(1) & O(1) & O(1) & O(h) & O(h) \\ O(1) & O(1) & O(1) & O(1) & O(h) & O(h) \\ O(1) & O(1) & O(1) & O(1) & O(1) & O(1) \\ O(1/h) & O(1/h) & O(1/h) & O(1/h) & O(1) & O(1) \\ O(1/h) & O(1/h) & O(1/h) & O(1/h) & O(1) & O(1) \\ O(1/h) & O(1/h) & O(1/h) & O(1/h) & O(1/h) & O(1/h) \end{pmatrix}, \tag{6.34}$$

The B-stability and accuracy estimations derived from the **BCS**analysis of the overspecified boundary conditions are very similar to those obtained for Factorizable Scheme # 1:

1) The scheme is B-unstable in a strict sense, but the instability affects only auxiliary variable ψ^h and only in a $O(h)$-small vicinity of the boundary. The scheme is B-stable in common integral norms.
2) With the exactly overspecified boundary conditions, the zone of $O(h)$ accuracy for ψ^h is two points adjacent to the outflow boundary (ψ_{N-2}^h and ψ_{N-1}^h). All other solution values converge with the second order as h tends to zero. The absence of a first-order convergence zone at the inflow is a result of cancellations implying $O(h^2)$-small coefficients c_4 and c_5.
3) Upon an arbitrary $O(h^2)$ perturbation of the overspecified data, the coefficients c_4 and c_5 become $O(h)$.

For practical boundary conditions, vectors $\mathbf{d}$ are the same as (6.18), (6.19). The **BCS**matrices,

$$\mathbf{BCS} = \begin{pmatrix} O(1) & 0 & O(h^2) & O(h^3) & 0 & 0 \\ 0 & O(1) & O(h) & O(h^2) & 0 & O(1) \\ 0 & O(1) & O(h) & O(h^2) & 0 & 0 \\ 0 & 0 & O(h) & O(h^2) & 0 & 0 \\ 0 & 0 & O(h) & O(h^2) & 0 & 0 \\ 0 & 0 & 0 & 0 & O(h^2) & 0 \end{pmatrix}, \tag{6.35}$$

for sets (B) and (C), and

$$\mathbf{BCS} = \begin{pmatrix} O(1) & 0 & O(h^2) & O(h) & 0 & 0 \\ 0 & O(1) & O(h) & O(1) & 0 & O(1) \\ 0 & O(1) & O(h) & O(1) & 0 & 0 \\ 0 & 0 & O(h) & O(1) & 0 & 0 \\ 0 & 0 & O(h) & O(1) & 0 & 0 \\ 0 & 0 & 0 & 0 & O(h^2) & 0 \end{pmatrix}. \tag{6.36}$$

for sets (D) and (E), guarantee B-stability for discrete problem (4.3) and second-order accuracy for sets (B) through (D). With set (E), the solutions converge with first-order rate.

Numerical tests have been performed for Scheme # 2 with the same parameters (6.22) and the same exact solution ($C_u = 1, C_p = 2$, and $\alpha = 7\pi$) as for Scheme # 1 in Section 6.1. Convergence of the discretization

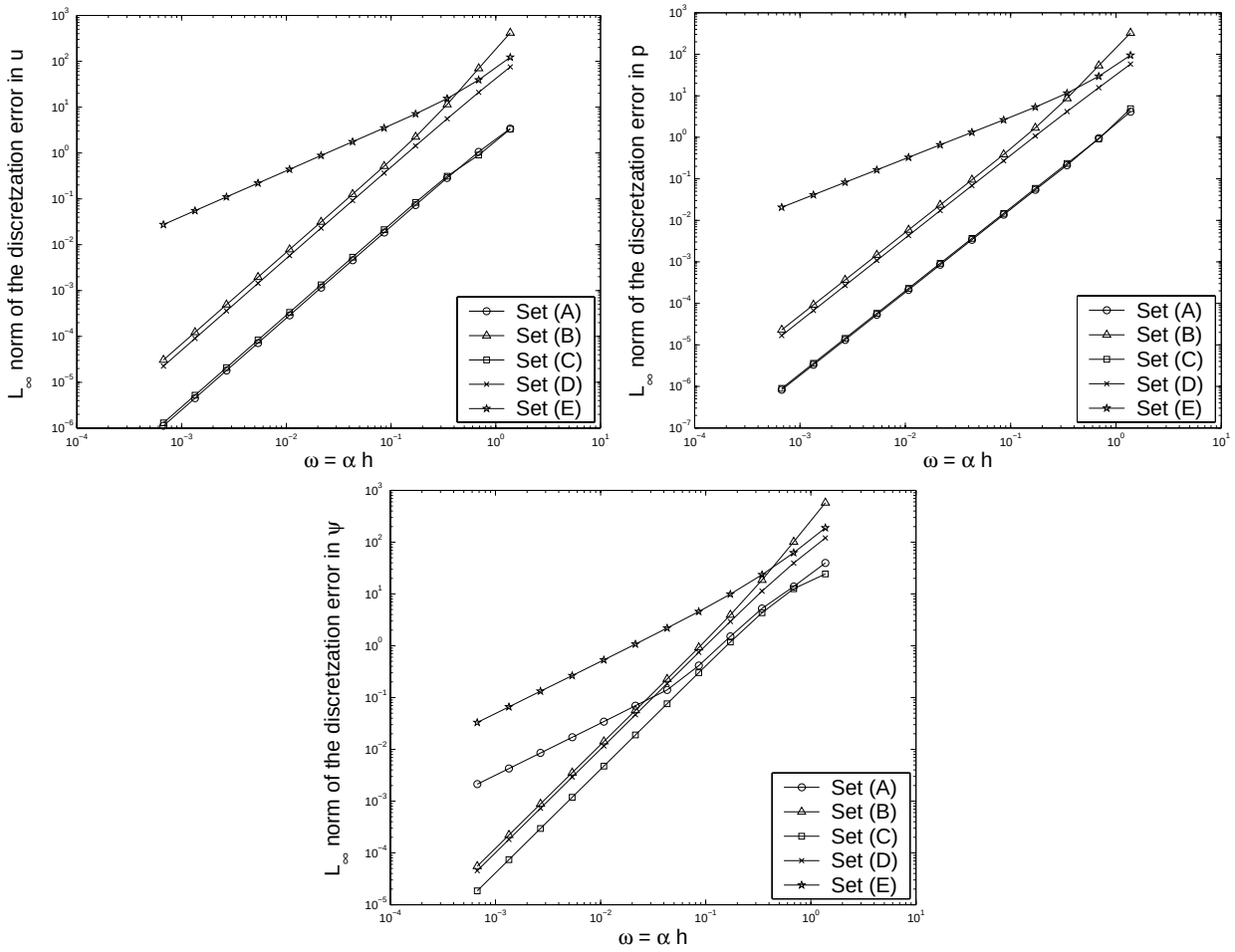

FIG. 6.2. *Scheme # 2: L_∞ norms of discretization errors in u, ψ, and p.*

errors in the L_∞ norm is demonstrated in Figure 6.2. The qualitative results confirm the predictions of the **BCS**analysis and are basically the same as in case of Scheme # 1:

1) The L_∞ norm of discretization errors in physical variables, u^h and p^h, is $O(h^2)$ for sets (A) through (D) of boundary conditions and is $O(h)$ for set (E).
2) The L_∞ norm of discretization errors in the auxiliary variable, ψ^h, is $O(h^2)$ for sets (B), (C), and (D) and is $O(h)$ for sets (A) and (E); for set (A), ψ^h is $O(h^2)$-small in any common integral norm.
3) The minimum discretization errors for physical variables are achieved with the overspecified boundary conditions.
4) Set (C) is the best among practical boundary conditions and very competitive with the overspecified boundary conditions.

Quantitative comparisons between Schemes # 1 and # 2 reveal that the discretization errors in physical variables, u^h and p^h, with Scheme # 2 are about two times smaller on the same grids.

7. Numerical Tests. This section reports results of numerical experiments performed for quasi-one-dimensional subsonic flow in a convergent-divergent channel. The nonconservative nonlinear differential

equations describing the problem are defined as

$$
\begin{aligned}
u\partial_x u + \tfrac{(\gamma-1)\epsilon}{p}\partial_x p &= 0, \\
\gamma p \partial_x u + u\partial_x p &= -\gamma p u \tfrac{\partial_x \sigma}{\sigma}, \\
(\gamma-1)\epsilon\partial_x u + u\partial_x \epsilon &= -(\gamma-1)\epsilon u \tfrac{\partial_x \sigma}{\sigma},
\end{aligned} \tag{7.1}
$$

where $\gamma = 1.4$ and $\sigma(x) = 1 - 0.8x(1-x)$ is the area distribution term. The physical boundary conditions

$$
\begin{aligned}
u(0) &= M(0)\left[\tfrac{1+\frac{\gamma-1}{2}}{1+M^2(0)\frac{\gamma-1}{2}}\right]^{\frac{1}{2}} &&= 0.53452, \\
p(1) &= \tfrac{1}{\gamma}\left[\tfrac{1+\frac{\gamma-1}{2}}{1+M^2(0)\frac{\gamma-1}{2}}\right]^{\frac{\gamma}{\gamma-1}} &&= 1.13984, \\
\epsilon(0) &= \tfrac{1}{\gamma(\gamma-1)}\left[\tfrac{1+\frac{\gamma-1}{2}}{1+M^2(0)\frac{\gamma-1}{2}}\right] &&= 2.04082
\end{aligned} \tag{7.2}
$$

corresponding to a flow with constant entropy and a Mach number of 0.5 at inflow and outflow, i.e., $M(0) = M(1) = 0.5$; the equations are nondimensionalized by density and speed of sound at the sonic condition. The Mach number distribution in the exact solution is shown on Figure 7.1.

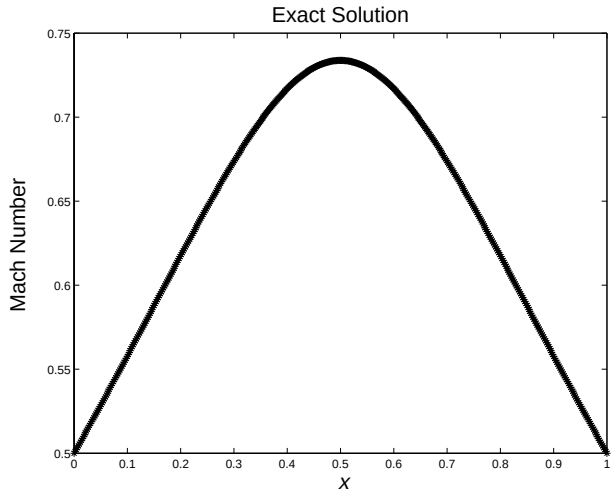

FIG. 7.1. *The Mach number distribution in the exact solution*

Discrete schemes approximating (7.1) in the interior belong to the family of factorizable schemes described as

$$
\begin{aligned}
u_j^h \partial^u u_j^h + \tfrac{(\gamma-1)\epsilon_j^h}{p_j^h}\partial^c p_j^h &= 0, \\
u_j^h \partial^u \psi_j^h - \mathcal{D}^h p_j^h &= 0, \\
\gamma p_j^h \partial^c u_j^h + \phi_j^h + u_j^h \partial^d p_j^h &= -\gamma p_j^h u_j^h \tfrac{\partial^c \sigma_j^h}{\sigma_j^h}, \\
(\gamma-1)\epsilon_j^h \partial^c u_j^h + u_j^h \partial^u \epsilon_j^h &= -(\gamma-1)\epsilon_j^h u_j^h \tfrac{\partial^c \sigma_j^h}{\sigma_j^h},
\end{aligned} \tag{7.3}
$$

where $\sigma_j^h = \sigma(jh)$. The boundary conditions related to the fourth (energy) equation are the physical boundary condition $\epsilon_0^h = \epsilon(0)$ and a numerical-closure equation corresponding to the first-order upwind discretization $\partial^u \epsilon_j^h$ in the discrete equation defined at $j = 1$. Six different discrete scheme have been tested for the other three equations:

1. Factorizable Scheme # 2 with a three-point discretization for the full-potential factor and overspecified boundary conditions.

2. Factorizable Scheme # 1 with a five-point discretization for the full-potential factor and overspecified boundary conditions.
3. Factorizable Scheme # 2 with a three-point discretization for the full-potential factor and set (C) of practical boundary conditions.
4. Factorizable Scheme # 1 with a five-point discretization for the full-potential factor and set (C) of practical boundary conditions.
5. Factorizable Scheme # 2 with a three-point discretization for the full-potential factor and set (B) of practical boundary conditions.
6. Factorizable Scheme # 1 with a five-point discretization for the full-potential factor and set (B) of practical boundary conditions.

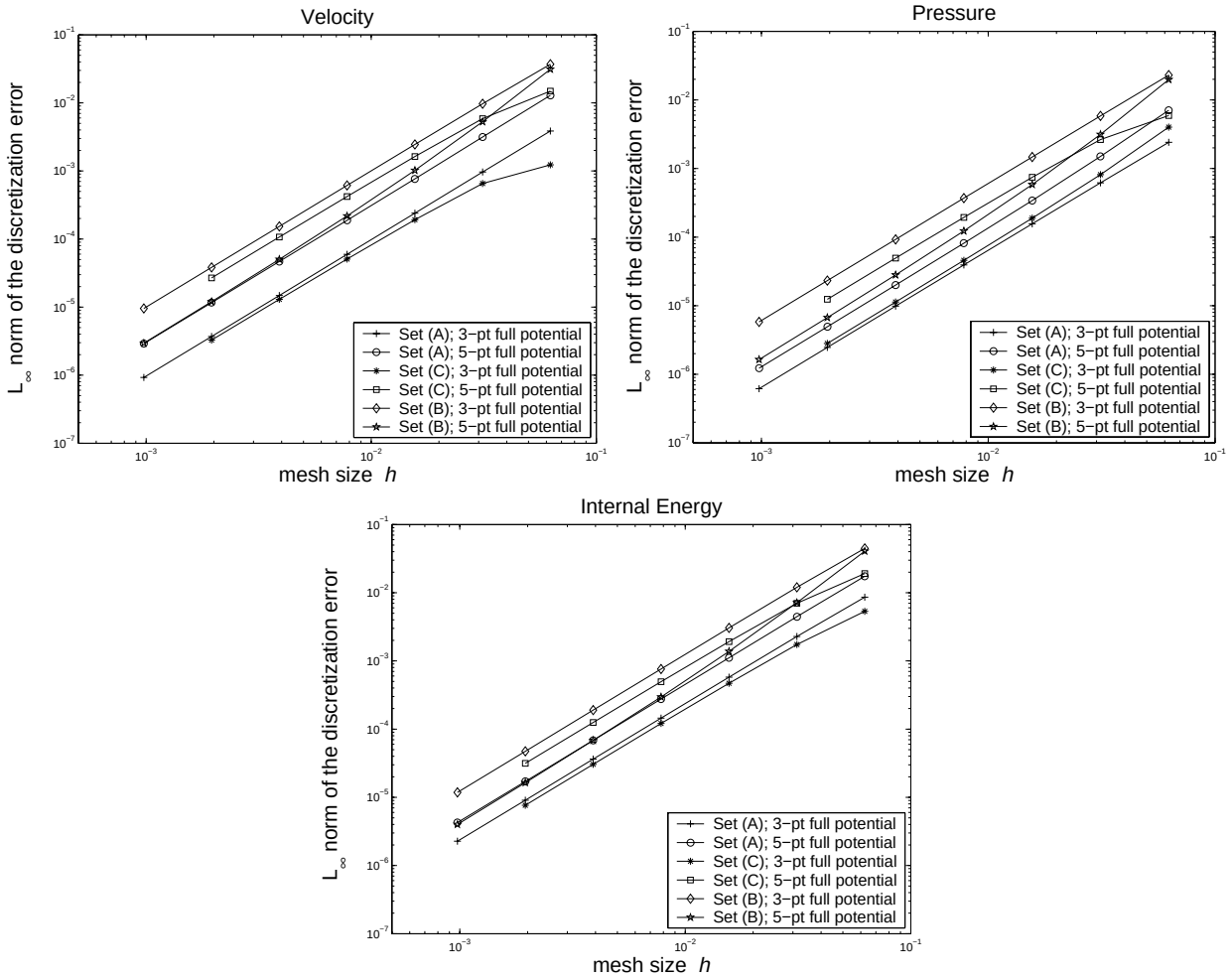

FIG. 7.2. *Nonlinear problem: L_∞ norms of discretization errors in u, p, and ϵ.*

The L_∞ norms of discretization errors are shown on Figure 7.2. In these tests performed for the nonlinear nonconservative Euler equations, the discretization-error history demonstrated by Scheme # 2 (3-point approximation for the full-potential operator) with Set (C) of practical boundary conditions is superior comparing to all other cases of practical boundary conditions and very close to the overspecified boundary conditions (Set (A)).

8. Conclusions and Further Research. Formulation of boundary conditions is a very important step in design of discretization schemes. The **BCS**analysis proved to be a very accurate and reliable tool in predicting the effect discrete boundary conditions have on B-stability and accuracy of discrete solutions. A general methodology for applying the **BCS**analysis to discretized well-posed constant-coefficient problem with a given set of boundary conditions includes the following steps:

1. Assume the exact solution of the target differential problem to be a Fourier component and compute right-hand side and boundary data.
2. Compute the discrete determinant operator. The stencil of the determinant operator determines the required number of boundary conditions at the inflow and outflow boundaries.
3. If the total number of boundary conditions (physical boundary conditions and numerical-closure equations) exceeds the required number, an equivalent set of boundary conditions should be formulated.
4. Compute the roots of the characteristic polynomial.
5. Find the normalized characteristic solutions.
6. Find particular and general solutions of the discrete problem.
7. Substitute the general solution into the tested set of boundary conditions and compute matrix $\mathbf{B}$ and vector $\tilde{\mathbf{d}}$.
8. Compute the **BCS**matrix and vector $\mathbf{d}$. To evaluate the asymptotic behavior of the **BCS**matrix as a function of mesh size h, one can invert matrices $\mathbf{B}$ numerically on several grids with different h and, then, compute entry-by-entry ratios of the numerical inverses.

Practical boundary conditions considered in this paper for second-order accurate factorizable discretizations are easy to implement and result in B-stable accurate discrete solutions. The **BCS**analysis and numerical tests have shown that for second-order accurate solutions, some of the numerical-closure equations must be second order. Optimization of practical boundary conditions may result in significant gains (of more than an order of magnitude) in the accuracy of discrete solutions on a given grid. Furthermore, practical boundary conditions may also have a positive effect on efficiency of multigrid solvers. It is expected that implementation of practical boundary conditions together with appropriate local procedures accompanying distributed relaxation should result in Laplace-like multigrid convergence for the Euler system of equations:

(1) TME is expected with multigrid solvers employing V-cycles rather than modifications of more expensive W- or F-cycles as in [9, 12, 18, 19, 20].

(2) Assuming very efficient solutions of convection operators (e.g., by marching), the overall convergence rates per an Euler-system distributed relaxation sweep is expected to be the same as the corresponding per-relaxation rates for the Laplace operator, e.g., 0.38 per sweep of lexicographic Gauss-Seidel relaxation within a V(1,1) cycle in a one-dimensional subsonic Euler problem with the second-order accurate three-point discretization for the full-potential factor. In a similar setting with overspecified boundary conditions, TME solvers with distributed relaxation and W or F cycles usually demonstrate convergence rates around 0.5 per relaxation.

Preliminary tests confirm the expected efficiency in solution of constant-coefficient model problems corresponding to the Euler system of equations.

The **BCS**analysis can be regarded as a generalization to systems of equations of the half-space discrete analysis [7, 10] that takes both the (inflow and outflow) boundaries into account. This connection implies that the **BCS**analysis can be used far beyond the task of boundary condition evaluation, e.g., for analyzing iterative solvers. It can be extended to multidimensional problems by considering the target discretization

on a layer bounded by two parallel hyper-planes. Solutions in the hyper-planes parallel to the boundaries are represented by one Fourier component in a time. In this way, the target multidimensional problem is translated into a one-dimensional problem, where the frequencies of the Fourier component are considered as parameters.

The applications of the **BCS**matrix analysis are extended far beyond the examples reported in this paper. It is a very instrumental in gaining insights about global effects some local conditions may have on solutions. The **BCS**matrix analysis plays a central role in adjusting the interior boundary conditions for the local procedures supplementing distributed relaxation. The main requirements for these boundary conditions is to prevent the local procedure from error magnifications because of the erroneous data unavoidable introduced at the interior boundary. The relative simplicity and effectiveness of the **BCS**analysis promise many further important applications.

REFERENCES

[1] A. Brandt, *Multi-level adaptive solutions to boundary-value problems.*, Math. Comp., 31 (1977), pp. 333–390.

[2] ——, *Guide to multigrid development*, in Multigrid Methods, W. Hackbusch and U. Trottenberg, eds., Lecture Notes in Math. 960, Springer-Verlag, Berlin, 1982.

[3] ——, *Multigrid techniques: 1984 guide with applications to fluid dynamics*, in Lecture Notes for the Computational Fluid Dynamics, Lecture Series at the Von-Karman Institute for Fluid Dynamics, The Weizmann Institute of Science, Rehovot, Israel, 1984. ISBN-3-88457-081-1, GMD-Studien Nr. 85, Available from GMD-AIW, Postfach 1316, D-53731, St. Augustin 1, Germany. Also available from Secretary, Department of Mathematics, University of Colorado at Denver, CO 80204-5300.

[4] ——, *Barriers to achieving textbook multigrid efficiency in CFD*, ICASE Interim Report 32, NASA CR-1998-207647, April 1998. Updated version available as Gauss Center Report WI/GC-10 at The Weizmann Institute of Science, Rehovot, Israel, December 1998.

[5] ——, *Appendix C: Recent developments in multigrid efficiency in computational fluid dynamics*, in Multigrid, Academic Press, London, 2000, pp. 573–589. Ulrich Trottenberg, C. W. Oosterlee, and A. Schüler.

[6] A. Brandt and N. Dinar, *Multi-grid solutions to elliptic flow problems*, in Numerical Methods for Partial Differential Equations, S. Parter, ed., Academic Press, New York, 1979, pp. 53–147.

[7] A. Brandt and B. Diskin, *Multigrid solvers for the non-aligned sonic flow: The constant coefficient case*, Computers and Fluids, 28 (1999), pp. 511–549. Also Gauss Center Report WI/GC-8 at The Weizmann Institute of Science, Rehovot, Israel, October 1997.

[8] A. Brandt, B. Diskin, and J. L. Thomas, *Textbook multigrid efficiency for computational fluid dynamics simulations*, AIAA Paper 2001-2570, 15th AIAA CFD Conference, Anaheim, CA, June 2001.

[9] A. Brandt and I. Yavneh, *On multigrid solution of high-Reynolds incompressible entering flow*, J. Comput. Phys., 101 (1992), pp. 151–164.

[10] B. Diskin and J. L. Thomas, *Half-space analysis of the defect-correction method for Fromm discretization of convection*, SIAM J. Sci. Comp., 22 (2000), pp. 633–655.

[11] B. Diskin and J. L. Thomas, *Distributed relaxation for conservative discretizations*, AIAA Paper 2001-2571, 15th AIAA CFD Conference, Anaheim, CA, June 2001.

[12] B. Diskin and J. L. Thomas, *New factorizable discretizations for the Euler equations*, ICASE Report 2002-6, NASA CR-2002-211456, April 2002.

[13] F. H. Harlow and J. E. Welch, *Numerical calculations of time-dependent viscous incompressible flow of fluid with free surface*, Physics of Fluids, 8 (1965), pp. 2182–2189.

[14] S. V. Patankar, *Numerical Heat Transfer and Fluid Flow*, Hamisphere Publishing Co./McGraw-Hill Co., New York, 1980.

[15] R. Peyret and T. D. Taylor, *Computational Methods for Fluid Flow*, Springer Verlag, New York, 1983.

[16] D. Sidilkover, *Factorizable scheme for the equation of fluid flow*, ICASE Report 99-20, NASA CR-1999-209345, June 1999.

[17] ——, *Some approaches toward constructing optimally efficient multigrid solvers for the inviscid flow equations*, Computers and Fluids, 28 (1999), pp. 551–571.

[18] J. L. Thomas, B. Diskin, and A. Brandt, *Distributed relaxation multigrid and defect correction applied to the compressible Navier-Stokes equations*, AIAA Paper 99-3334, 14th Computational Fluid Dynamics Conference, Norfolk, VA, July 1999.

[19] ——, *Textbook multigrid efficiency for the incompressible Navier-Stokes equations: High Reynolds number wakes and boundary layers*, Computers and Fluids, 30 (2001), pp. 853–874. Also ICASE Report 99-51 (NASA CR-1999-209831), December 1999.

[20] J. L. Thomas, B. Diskin, A. Brandt, and J. C. South, *General framework for achieving textbook multigrid efficiency: Quasi-1-d Euler example*, in Frontiers of Computational Fluid Dynamics — 2002, D. A. Caughey and M. M. Hafez, eds., World Scientific Publishing Company, Singapore, 2002, pp. 61–79. Also ICASE Report 2000-30, NASA/CR-2000-210320.

REPORT DOCUMENTATION PAGE

Form Approved
OMB No. 0704-0188

1. AGENCY USE ONLY *(Leave blank)*	2. REPORT DATE	3. REPORT TYPE AND DATES COVERED
	May 2002	Contractor Report

4. TITLE AND SUBTITLE
Analysis of boundary conditions for factorizable discretizations of the Euler equations

5. FUNDING NUMBERS
C NAS1-97046
WU 505-90-52-01

6. AUTHOR(S)
Boris Diskin and James L. Thomas

7. PERFORMING ORGANIZATION NAME(S) AND ADDRESS(ES)
ICASE
Mail Stop 132C
NASA Langley Research Center
Hampton, VA 23681-2199

8. PERFORMING ORGANIZATION REPORT NUMBER
ICASE Report No. 2002-13

9. SPONSORING/MONITORING AGENCY NAME(S) AND ADDRESS(ES)
National Aeronautics and Space Administration
Langley Research Center
Hampton, VA 23681-2199

10. SPONSORING/MONITORING AGENCY REPORT NUMBER
NASA/CR-2002-211648
ICASE Report No. 2002-13

11. SUPPLEMENTARY NOTES
Langley Technical Monitor: Dennis M. Bushnell
Final Report
To be submitted to the SIAM Journal on Scientific Computing.

12a. DISTRIBUTION/AVAILABILITY STATEMENT
Unclassified–Unlimited
Subject Category 64
Distribution: Nonstandard
Availability: NASA-CASI (301) 621-0390

12b. DISTRIBUTION CODE

13. ABSTRACT *(Maximum 200 words)*
In this article, several sets of boundary conditions or factorizable schemes corresponding to the steady-state compressible Euler equations are evaluated. The analyzed model is a one-dimensional constant-coefficient problem. Numerical tests have been performed for a fully subsonic quasi-one-dimensional flow in a convergent/divergent channel.

This paper focuses on the effect of boundary-condition equations on stability and accuracy of the discrete solutions. Explicit correspondence between solutions and boundary conditions is established through a boundary-condition-sensitivity (BCS) matrix. The following new findings are reported:
(1) Examples of stable discrete problems contradicting a wide-spread belief that employment of a one-order-lower approximation schemes in an O(h)-small region does not affect the overall accuracy order of the solution have been found and explained. Such counterexamples can only be constructed for systems of differential equations. For scalar equations, the conventional wisdom is correct.
(2) A negative effect of overspecified (although, exact) boundary conditions on accuracy and stability of the solution has been observed and explained.
(3) Sets of practical boundary conditions for factorizable schemes providing stable second-order accurate solutions have been formulated. These schemes belong to a family of second-order schemes requiring second-order accuracy for some numerical-closure boundary conditions.

14. SUBJECT TERMS	15. NUMBER OF PAGES
compressible Euler equations, factorizable discretization scheme, practical boundary conditions, I-stability, B-stability	31
	16. PRICE CODE A03

17. SECURITY CLASSIFICATION OF REPORT	18. SECURITY CLASSIFICATION OF THIS PAGE	19. SECURITY CLASSIFICATION OF ABSTRACT	20. LIMITATION OF ABSTRACT
Unclassified	Unclassified		